이학석사 학위논문

지난 마지막 간빙기 이후 동해 서부의 알케논 수온 변화 복원

Past sea surface temperature of the western part of the East Sea since the last interglacial period

지도교수 이 경 은

2008년 8월

한 국 해 양 대 학 교 대 학 원

해양생명환경학과

최 지 영

Table of Contents

List of figures

List of appendix

지난 마지막 빙하기 이후 동해 서부의 알케논 수온 변화 복원

최 지 영

한국해양대학교 해양환경학전공

초 록

이 논문의 목적은 지난 130,000년 동안 동해의 해양 환경의 변화를 재건하는 것이다. 해양 환경 변화의 재건을 위해 동해의 서쪽 가장자리(margin)에서 채취 한 세 개의 피스톤 코어 (05PC-14, 05PC-15, 05PC-23)에서 C_{37} 알케논 농도를 측정하고, 이로부터 과거 동해에서의 표층수온을 계산하였다. 표층수온은 $U^{K'}_{37}$ = 0.034T + 0.039 (Prahl et al., 1988)을 이용하여 계산하였다. 각 코어의 연대결정은 이미 연대를 알고 있는 다른 피스톤 코어 (05PC-21, MD01-2407)와의 L*(lightness) 값의 비교를 통해 이루어졌다. $U^{K'}_{37}$으로 계산된 표층수온은 130,000년 동안 크게 변동하는 것을 볼 수 있었다. Marine Isotope Stage (MIS) 5 (71,000 ~ 130,000년 전)는 지난 마지막 간빙기에 해당하는 시기이다. MIS 5동안 각 코어별로 표층 수온의 변화를 살펴보면, 05PC-14에서는 MIS 5a동안 16.6℃에서 12.8℃로 수온이 감소하였다. 05PC-15에서는 MIS 5e에서 최고값 23.3℃, MIS 5a에서 최소값 13.8℃를 보였고, 05PC-23에서는 MIS 5e에서 25.8℃의 최고값, MIS 5a에서 9.6℃의 최소값을 나타냈다. MIS 4 (57,000-71,000년 전)와 MIS 3 (29,000-57,000년 전)는 빙하기에 해당한다. MIS 4동안에 동해의 표층 수온 변화는, 05PC-14에서는 10.6-12.7℃, 05PC-15에서는 12.4-14.9℃, 05PC-23에서는 9.5-14℃로 모두 15℃이하의 낮은 수온 값을 보였다. MIS 3동안 표층 수온 변화는, 05PC-14에서는 8.5-15.7℃로 비교적 낮은 수온 분포를 보였다. 이에 반해 05PC-15에서는

15.1-27.4℃, 05PC-23에서는 14.9-25.7℃로 두 코어에서는 간빙기에 해당하는 MIS 5a 동안의 표층 수온보다 높은 값을 보였다. MIS 2 (15,000-29,000년 전)는 지난 마지막 빙하기에 해당한다. MIS 2 전기와 중기동안에는 알케논 농도가 낮아서 수온을 계산할 수 없었다. MIS 2 후기에는 05PC-14에서는 13.8-16℃, 05PC-15에서는 13-25.4℃, 05PC-23에서는 12.5-18.2℃의 수온분포를 보였다. 이 시기 동안의 표층 수온은 빙하기에 해당함에도 불구하고 세 코아 모두 간빙기인 MIS 5a 동안의 표층 수온보다 높은 값을 보였다. MIS 1 (0-15,000년 전)는 간빙기에 해당한다. MIS 1 동안의 동해 표층 수온의 변화는, 05PC-14에서는 15.1-19.4℃, 05PC-15에서는 15.1-21.6℃, 05PC-23에서는 15.7-17.6℃로 나타났다.

동해에서의 표층 수온 변화는 아시아 몬순의 변화와 해수면 변동에 따른 쓰시마 해류 유입의 변화와 밀접한 관계가 있다. MIS 5동안에는 MIS 5e에서 MIS 5a로 갈수록 수온이 서서히 감소하는 경향을 보였다. MIS 5a와 5b 동안의 표층 수온은 현재의 표층 수온에 비해 2~3℃정도 낮았다. 이는 MIS 5a와 5b 동안 여름몬순의 세기는 조금씩 약화되고 상대적으로 겨울 몬순은 강화되면서 일어난 기후변화에 의한 현상일 것으로 생각된다. 또한 해수면 변화로 인해 동해로의 난류유입이 약화되면서 수온 감소에 영향을 미쳤을 것으로 생각된다. MIS 4 동안에는 빙하가 강화되면서 전 세계 해수면이 60-80m 가량 낮아졌다고 보고되어졌다. 이로 인해 얕은 해협을 통해 동해로 유입되던 따뜻한 쓰시마 해류의 흐름이 제한되었을 것이고, 강화된 겨울 몬순도 이 시기의 낮은 수온에 상당한 영향을 미쳤을 것이다. MIS 3동안에는 MIS 4 동안의 수온에 비하여 높은 수온을 보였다. MIS 3동안 높은 수온을 보이는 것은 당시 60-80m 가량의 해수면 하강으로 인하여 쓰시마 난류 유입이 제한되었고 겨울 몬순이 강화되었던 빙하기 동안의 상황을 고려해 보면 매우 이례적인 현상이다. 이런 갑작스런 수온 상승은 MIS 3 중반 무렵에 나타났으며, 시기에서는 알케논 농도의 급격한 증가도 확인할 수 있었다. 이에 해당하는 코아 깊이에서는 암엽리층(Dark Laminated Mud, DLM)을 확인 할 수 있었다. 암엽리층은 바닥의 강한 혐기성 환경으로 인하여 유기물 분해가 제한되면서 발생한다 (Demasion and Moore., 1980). 따라서 MIS 3 중기에 동해는 강한 혐기성 환경으로 인하여 암염리층이 나타났으며, 이는 이 시기 동안 알케논 농도의 증가를 뒷받침한다. 그러나 이는 MIS 3 동안의 높은 수온을 설명하기에는 부족하다. MIS 2 동안에도 세 코아 모두에서 15℃이상의

높은 수온을 보였다. MIS 2에서의 높은 수온은 이전의 여러 논문에서도 발표된 바가 있다. 하지만 이에 대한 명백한 원인이 아직 밝혀지지 않았다. 따라서 15,000~60,000년 전 사이의 빙하기 동안 동해에서의 이례적인 높은 수온의 원인에 대해서 아래에서 더 자세히 살펴본다. 마지막으로 MIS 1은 간빙기에 해당하며 세 코어 모두에서 수온이 15~18℃로 현재와 유사한 수온 분포를 나타냈다. 이는 여름 몬순의 강화와 쓰시마 해류가 동해로 재유입이 되면서 영향을 받은 것으로 보인다.

빙하기 동안 나타난 높은 수온에 영향을 미칠 수 있는 요인들에 대해서 생각해 보았다. 첫 번째로 알케논 생산자의 구성 변화이다. 이 전 연구들에 따르면 *G. oceanica*로부터 계산된 수온이 *E. huxleyi*의 것보다 더 높게 나타나는 것을 확인했다. 따라서 지난 빙하기 동안 동해의 알케논 생산자가 현재와는 다르게 *G. oceanica*가 주 생산자였다면 본 논문에서 계산된 알케논 수온은 당시 수온보다 더 높게 계산되었을 가능성이 있다. 두 번째 가능성은 염분의 영향이다. 최근 Rosell-Melé, (1998)은 C_{37} 알케논의 전체 양에 대한 $C_{37:4}$의 상대적인 양 (37:4%)이 5보다 큰 지역은 6℃ 이하의 수온을 나타낸다고 추정하였다. 본 논문에서 사용한 세 코아 (05PC-14, 05PC-14, 05PC-23)에서는 빙하기 동안 37:4%의 값은 5에는 전혀 미치지 못했다. Rosell-Melé, (1998)의 관점에 따르면, 세 코아의 빙하기 동안의 수온은 적어도 6℃보다는 높았다는 것을 의미한다. 세 코아에서 알케논으로부터 계산된 빙하기 동안의 수온 값이 약 15℃ 이상 이였다는 점을 고려하면, 염분의 변화는 빙하기 동안의 높은 수온 값에 대한 직접적인 증거가 되지 못한다. 하지만 이에 대한 좀 더 확실한 증거를 수반하는 연구가 앞으로 더 진행되어야 할 것이다. 세 번째 가능성은 $U^{K'}_{37}$ 값에 대한 영양염 농도 변화의 영향이다. Epstein et al. (1998)의 연구에 따르면, 영양염 농도의 40μM에서 1μM 미만으로 감소는 $U^{K'}_{37}$ 값을 0.10-0.19 가량 증가시키며, 이는 1.8-4.4℃의 수온 상승을 의미한다. 빙하기 동안 동해는 강한 성층의 발달로 심층에서 표층으로의 영양염 이동이 제한되어 표층에서의 영양염 농도는 현저히 낮았을 것으로 생각된다. 하지만 이것만으로는 당시의 영양염 농도 변화를 설명하기에는 부족하다. 따라서 $U^{K'}_{37}$ 값에 대한 영양염 농도 변화의 영향에 대해 설명하기 위해서는 빙하기-간빙기 동안 동해에서의 영양염 농도의 변화에 대한 연구가 우선되어야 할 것이다.

Past sea surface temperature of the western part of the East Sea since the last interglacial period

Ji Young Choi

Division of Marine Environment and Bioscience, Korea Maritime University, Busan, 606-791, Korea

Abstract

The purpose of this paper is to reconstruct the detailed paleoceanographic history of the East Sea during 130-kyr. Three piston cores 05PC-14, 05PC-15 and 05PC-23 taken from the western margin of the East Sea were examined. In this study, the C_{37} alkenone content were measured, and past sea surface temperature (SST) was calculated using $U^{K'}_{37}$ = 0.034T + 0.039 (Prahl et al., 1988). The age of the sediment cores was determined by the direct correlation of lightness (L*) to well-dated core MD01-2407 in Oki Ridge and 05PC-21 in Korea Plateau, with a comparition of well-known lithostratigraphic and tephrostratigraphic markers. Alkenone-based SST from the core sediments showed that the past SST fluctuated greatly. In core 05PC-14, the temperature decreased from 16.6℃ to 12.8℃ during the period of marine isotope stage (MIS) 5a. Then, the temperature fluctuated between 8.5℃ and 15.7℃ during MISs 3 and 4. Due to the low alkenone contents, $U^{K'}_{37}$ values could not be calculated during the MIS 2. After that, it continued to fluctuate between 13.8℃ and 19.4℃. In core 05PC-15, the temperature decreased from 23.3℃ to 13.8℃ during MIS 5. Then,

the temperature fluctuated between 12.4℃ and 19℃. During the MIS 3, it was anomalously high, which fluctuated between 15.1℃ and 27.4℃. During the MIS 2, alkenone temperature was not calculated due to the low alkenone contents. After that, it fluctuated between 13.8℃ and 25.4℃. In core 05PC-23, the temperature decreased from 25.8℃ to 9.6℃ during MIS 5. Then, the temperature fluctuated between 9.6℃ and 12.3℃ during MIS 4. However, during the MIS 3, the temperature was abnormally warm. It was scattered between 15℃ and 25.8℃. Due to the low alkenone contents, $U^{K'}_{37}$ values could not be calculated during the MIS 2. After that, it continued to fluctuate between 15.7℃ and 18.2℃.

Variation in the SST of the East Sea is considered to be closely related to changes in the east asian monsoon system and global sea level. For period of MIS 5, the alkenone temperatures gradually decreased from MIS 5e to MIS 5a. Especially, during MISs 5a and 5b, alkenone temperature was lower than those of present. It seems that lower SST was influenced by weaker summer monsoon and/or stronger winter monsoon than those of present. Also, sea level fall of 60m (Lambeck et al. 2002) would be restricted influx of warm water. According to Tada et al. (1999), the relative contributions of the Tsushima Warm Current (TWC) and East China Sea Coastal Water (ECSCW) varied significantly during this time interval. Therefore, most of the alkenone components would be when a strong influx of ECSCW would have supplied enough nutrients to sustain high surface productivity. Temperature of ECSCW is relatively lower than those of TWC. As a result, strong inflow of ECSCW into the East Sea could induce the lower SST of MISs 5a and b than those of MIS 1.

For period of MIS 4, the alkenone temperatures were very low. It seems to be closely associated with a global sea level fall of 60-80m during this period, which restricted the inflow of the TWC into the East Sea. Also, the low SSTs were

influenced by strong winter monsoon during this period.

For period of MIS 3, $U^{K'}_{37}$-derived temperatures were relatively higher than those of MIS 4. Considering a global sea-level fall of 60-80m (Waelbroeck et al., 2002) and strong winter monsoon (Wang et al., 2005) during the last glaciation, warm alkenone temperature during the MIS 3 would be anomalous. Abruptly increasing SST was at middle MIS 3 (about 50 kyr BP; 10.6℃ to 14.1℃ in 05PC-14, 17.4℃ to 27.4℃ in 05PC-15, and 14.9℃ to 25.7℃ in 05PC-23). The alkenone contents also increased at same period (0.3μg/g to 3.3μg/g in 05PC-14, 0.1μg/g to 1.2μg/g in 05PC-15, and 0.4μg/g to 5.5μg/g in 05PC-23). The core depth including abruptly high alkenone temperature in middle MIS 3 was showed Dark Laminate Muds (DLM). DLM was caused by bottom water anoxic condition owing to water-column stratification (Demasion and Moore, 1980). Tada et al. (1999) suggested that during the glacial period of low sea level (-60 ~ -90m), bottom water condition was anoxic. It seems that anoxic bottom water condition influenced abruptly high alkenone contents during the MIS 3, but it is insufficient that why alkenone temperature abruptly increase during the MIS 3.

For period of MIS 2, some alkenone temperature were also anomalously high. It has been reported previously for the East Sea, but it's not clear for what to be a major factor responsible for the anomalously warm alkenone temperature. Further studies are necessary.

For period of MIS 1, alkenone temperature increased up to the present temperature in the early MIS 1. It seems to be closely related to global sea level changes, which influenced the warm water inflow into the East Sea during the mid MIS 1 (8-10 kyr BP), and change of the East Asian monsoon system.

Anomalously high alkenone temperatures occurred repeatedly during glacial period between 15 and 60 kyr BP. These warm alkenone temperature episodes

would have had multiple causes. Such warm alkenone temperature events in the glacial period have three possible causes. The first possibility is an effects of haptophyte species on alkenone-SSTs. The second possibility is a salinity effects on alkenone-SSTs. The third possibility is an effect of nutrient concentration and growth rate on alkenone-SSTs. These effects together could have caused anomalously warm alkenone temperatures in the glacial period in the study area of 05PC-14, 05PC-15 and 05PC-23. More investigations are necessary to understand what happened in western margin of the East Sea at the time of 15-60 kyr BP.

1. Introduction

Paleoceanographic conditions in the East Sea drastically changed during the Late Quaternary. A number of the studies have revealed the paleoceanographic history of the East Sea using foraminiferal oxygen isotopes (Oba et al., 1991, 1995; Keigwin and Gorbarendo, 1992), alkenone SST reconstructions (Ishiwatari et al., 2001; Fujine, 2004; Lee, 2007) and geochemical analysis (Masuzawa and Kitano, 1984; Crusius et al., 1999; Tada et al., 1999).

The Marine Isotope Stage (MIS) 2 is the late glacial period between 15 and 29 kyr BP. During the MIS 2, the global sea level was lowered by approximately 120-130m, and then the inflow of the warm and saline Tsushima Warm Current (TWC) into the East Sea was restricted (Oba et al., 1991; Keigwin and Gorbarendo, 1992). Instead, fresh water input such as precipitation probably dominated in the area at this period (Keigwin and Gorbarendo, 1992). As the sea level of the East Sea fall, the paleoceanographic conditions in the East Sea substantially changed. Lee (2007) presented SST and SSS variations during the glacial period in the Ulleung Basin using alkenone temperature and oxygen isotopic composition. This study indicated that the oxygen isotopic ratio of planktonic foraminifer shifted to lighter values during the glacial period. Oba et al. (1991) and Gorbarenko and Southon. (2000) also presented that the East Sea had the very low $\delta^{18}O$ values of planktonic foraminifera during the glacial period. This result is different from heavier isotopic ratio of the global ocean.

According the Greenland $\delta^{18}O$ records of the GISP2 ice core (Grootes and Stuicer, 1997), oxygen values was heavier during the glacial period. The light oxygen isotopic value of the East Sea during the glacial period was related to the East Sea level fall. As a result, Sea Surface Salinity (SSS) of the East Sea decreased drastically. The low salinity surface water during this period increased the stability of the water column. This led the bottom water to strong anoxic sedimentary conditions (Crusius et al., 1999).

The MISs 3 and 4 are the last glaciation period between 29 and 71 kyr BP. Ikehara (2003) presented results from the ice rafted debris (IRD) in core from the northeastern part near Hokkaido. This study indicated that during the MIS 3 and 4, southern margin of sea ice might have moved southward, and the East Sea experienced cooling and decreased sea-surface salinity. Based on this observation, the East Sea has experienced weak ventilation due to reduced SSS during this period. Tada et al. (1999) suggested increased influx of the East China Sea Coastal Water (ECSCW). It is evidence which is a low-salinity coastal water diatom characteristic of the ECSCW. These studies indicated that weak stratification of the water column also might have resulted from relatively low sea level and an increase in net fresh water influx during these periods.

MIS 5 is the last interglacial period between 71 and 130 kyr BP. It is unlikely that changes of the East Sea temperature during the MIS 5 period. Lambeck et al. (2002) estimated the global sea-level change using the global change in ocean and ice volumes for the time interval. This study suggested that the global sea-level change was approximately 60m below

during MIS 5. Despite sea-level low of 60m, it was enough for TWC to flew into the East Sea. Irino and Tada (2002) reported that millennial scale variability of the East Sea temperature during the MIS 5 was controlled by high-frequency variation between summer monsoon and winter monsoon. However, Asian monsoon system was not simple variation patterns. Rather, further study is necessary.

In this study, main question is that how the current system changed and how paleoceanography condition responded to global climate change in the East Sea during the 130 kyr. Especially, the western margin of the East Sea is important because Liman Cold Current (LCC) flows southward along the western boundary and Tsushima Warm Current (TWC) also flows northward along the western boundary. However, studies of the western margin of the East Sea are insufficiency. Therefore, further research of the western margin of the East Sea is necessary to define palaeoceanography condition change of the East Sea. In this study, we used the alkenone unsaturation index to investigate changes in SST in the western margin of the East Sea during the 130 kyr. We used sediment material from three piston cores (05PC-14, 05PC-15, and 05PC-23) collected from the bathymetric high of the South Korea Plateau. The sediments of 05PC-15 and 05PC-23 cores cover up to the period MIS 5e. The sediments of 05PC-14 core cover up to the period MIS 5a. We measured the C_{37} alkenone content and calculated past SST from the alkenone values. Based on the reconstruction of past SSTs, we discuss the paleoenvironmental changes of the East Sea during the last interglacial period.

3. Background of using alkenone as a proxy of sea surface temperature

Long-chain methyl ketones with two to four double bonds (alkenones) are biosynthesized by some algae of the class Haptophyceae / Prymnesio -phyceae, such as *Emiliania huxleyi*. *E. huxleyi* is the most abundant and widespread coccolithophorid in the oceans and is most probably the main producer of alkenones found in recent sediments. Brasell et al. (1986) primarily introduced the ketone unsaturation index U^{K}_{37} :

$$U^{K}_{37} = \frac{[37:2] - [37:4]}{[37:2] + [37:3] + [37:4]}$$

U^{K}_{37} is calculated from the relative abundances C_{37} methyl alkenones containing 2-4 double bond. But the tetra-unsatured alkenone ($C_{37:4}$) which becomes more significant with decreasing temperature is not always present in particulate matter and sediments. Therefore, Prahl and Wakeham. (1987) suggested to use the simpler equation without the $C_{37:4}$ component, the simplified unsaturation index $U^{K'}_{37}$:

$$U^{K''}_{37} = \frac{[37:2]}{[37:2] + [37:3]}$$

Prahl and Wakeham (1987) calibrated the response of unsaturation in the long-chain alkenones to growth temperature using laboratory cultures of a single strain of *E. huxleyi*. $U^{K'}_{37}$ has proven to be a useful indicator of past sea surface temperature. The calibration curve of a simplified unsaturation index $U^{K'}_{37}$ was shown to be remarkably linear over the range of growth temperatures examined. The linear relationship has derived past

sea surface temperature from $U^{K'}_{37}$ = 0.034T + 0.039 (Prahl et al., 1988). Alkenones paleothermometry has been applied to numerous studies on the reconstruction of past temperature. Past SST has been calibrated using results of analysis of water column and sediment trap samples (using $U^{K'}_{37}$, Lee and Schneider., 2005; Rosell-Melé et al., 2000) and surface sediments (using $U^{K'}_{37}$, Müller et al., 1998). These studies show the validity of the culture calibration for the open ocean.

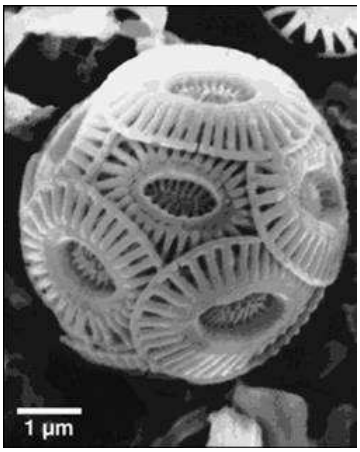

Fig. 1. ***Emiliania huxleyi***

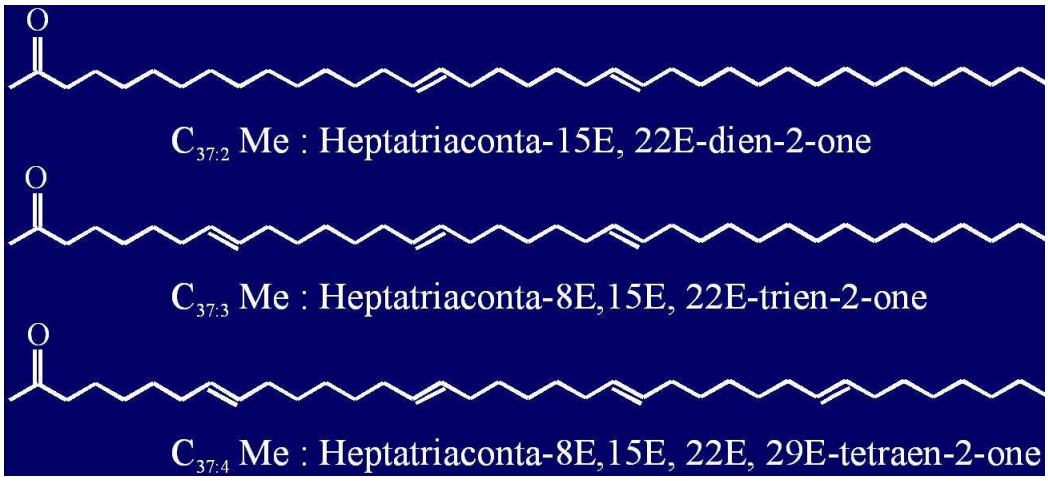

Fig. 2. Three types of C_{37} alkenones

3. Modern hydrography in the East Sea

The East Sea is a semi-enclosed marginal sea located on the mid-latitude eastern margin of the Eurasian continent. Water depths of the East Sea range from less than 2000m in the south to more than 3700m in the north. The average water depth is about 1350m. The East Sea is connected with the East China Sea to the south, Pacific Ocean to the east, and Okhotsk Sea to the north only through narrow and shallow (<130m) straits (Korea strait, Tsugaru Strait, Soya Strait, and Tartar Strait; Fig. 1). At present, the Tsushima Warm Current (TWC) and the Liman Cold Current (LCC), which are associated with the subtropical and subarctic circulations in the North Pacific respectively, are two major currents in the East Sea, and divide the East Sea into warm (southern) and cold (northern) regions with the boundary (Polar front) around 40°N. The TWC, which is a branch of the Kuroshio Current, flows into the East Sea through the Korea Strait and flows out through the Tsugaru and Soya Straits. TWC is characterized by high temperature and high salinity. Moreover, TWC transports a small amount of East China Sea Coastal Water (ECSCW) and/or Yellow Sea water, which is a lower salinity and higher organic matter, into the East Sea. The LCC, which is a branch of the Kuril Current, flows southward along the North Koran and Siberian coasts. LCC is characterized by low temperature and low salinity. It then forms a cyclonic gyre north of the subpolar front (Senjyu and Sudo 1994; Isobe and Isoda 1997). Also, LCC is known to be driven by the wind with positive stress curl and surface

cooling. These currents is associate largely with change of SST in the East Sea.

The changes of the SST in the East Sea are also related to the atmosphere-ocean circulation regime of the Northern Hemisphere. Especially, Asian monsoon is a climate system involving interactions between land and ocean (Yasunari, 1991). During the summer monsoon, much of the region falls under the influence of the Ogazawa high with its warm and moisture-laiden southwesterly winds. In winter, development of the Siberian High and Aleutian Low, and the East Asian jet stream are intimately connected with strong winter monsoon (Webster, 1987). Therefore, during the summer monsoon, the East Sea is influenced by warm and moisture wind from the Pacific to the Asian continent. Whereas, during the winter monsoon, the East Sea is influenced by cold and dry air masses blowing from the Siberian high to the surrounding lows. Rather, the East Sea climate is chiefly controlled by the winter and summer monsoons. Present seasonal SST and SSS data of the East Sea from NOAA are showed in Fig. 3 and Fig. 4. The mean values of water temperature and salinity are 6-10℃, and 34.2‰, respectively, in winter. In summer, the surface water is characterized by high temperature and low salinity. The mean values of SST and SSS are 20-24℃ and 33.4‰, respectively, in summer. The annual average SST and SSS is 15℃ and 33.5‰, respectively. The seasonal variation in SST is closely related to the wind system and East Asian monsoon. The seasonal variation in SSS is closely related to dilution by river discharge from the adjacent land.

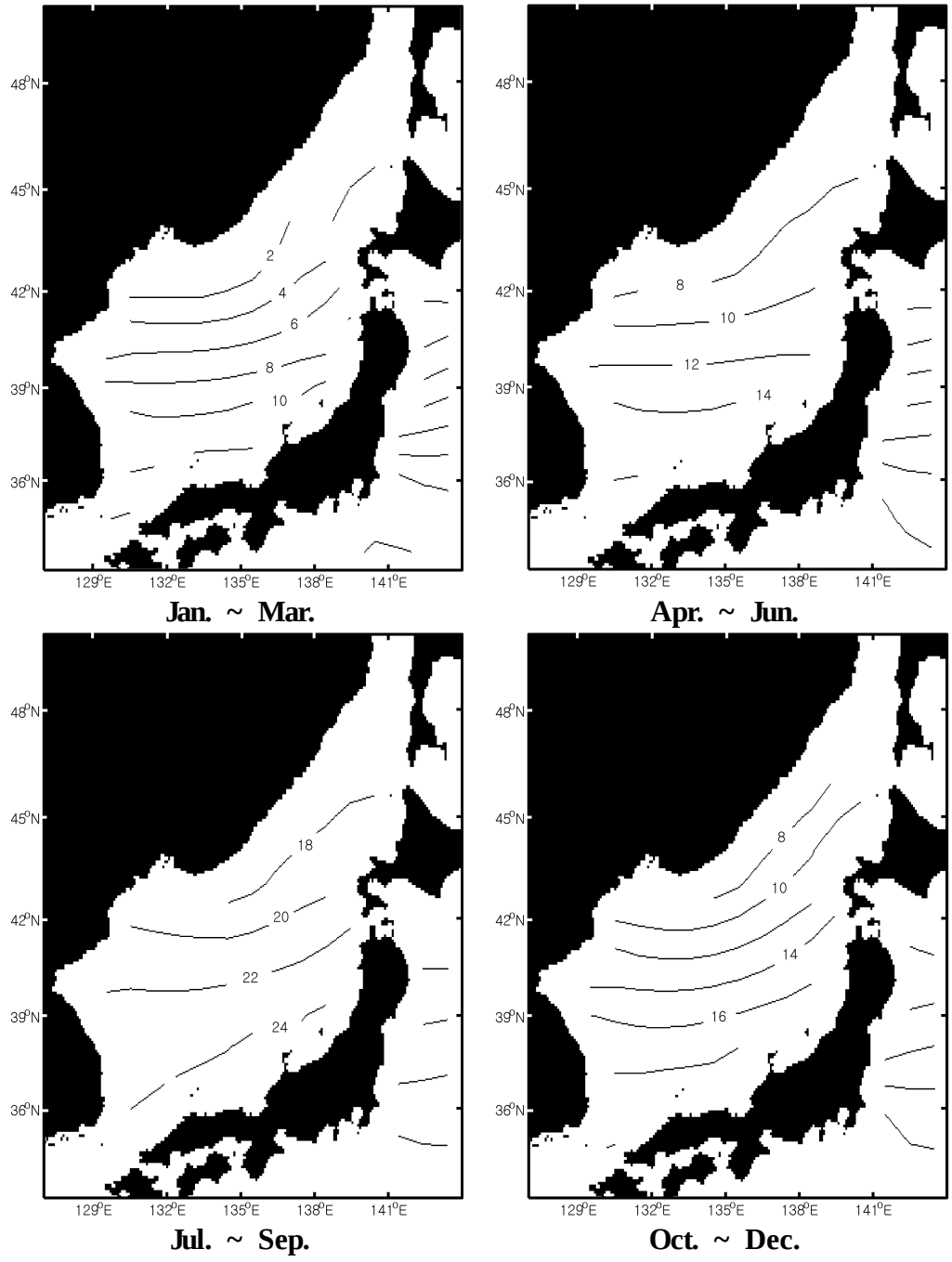

Fig. 3. Modern seasonal surface temperature distributions (℃) over in the East Sea. The SST data were downloaded from the web site http://iridl.ldeo.columbia.edu/SOURCES/.NOAA/.NODC/.WOA98/.SEASONAL/.analyzed/.temperature/.

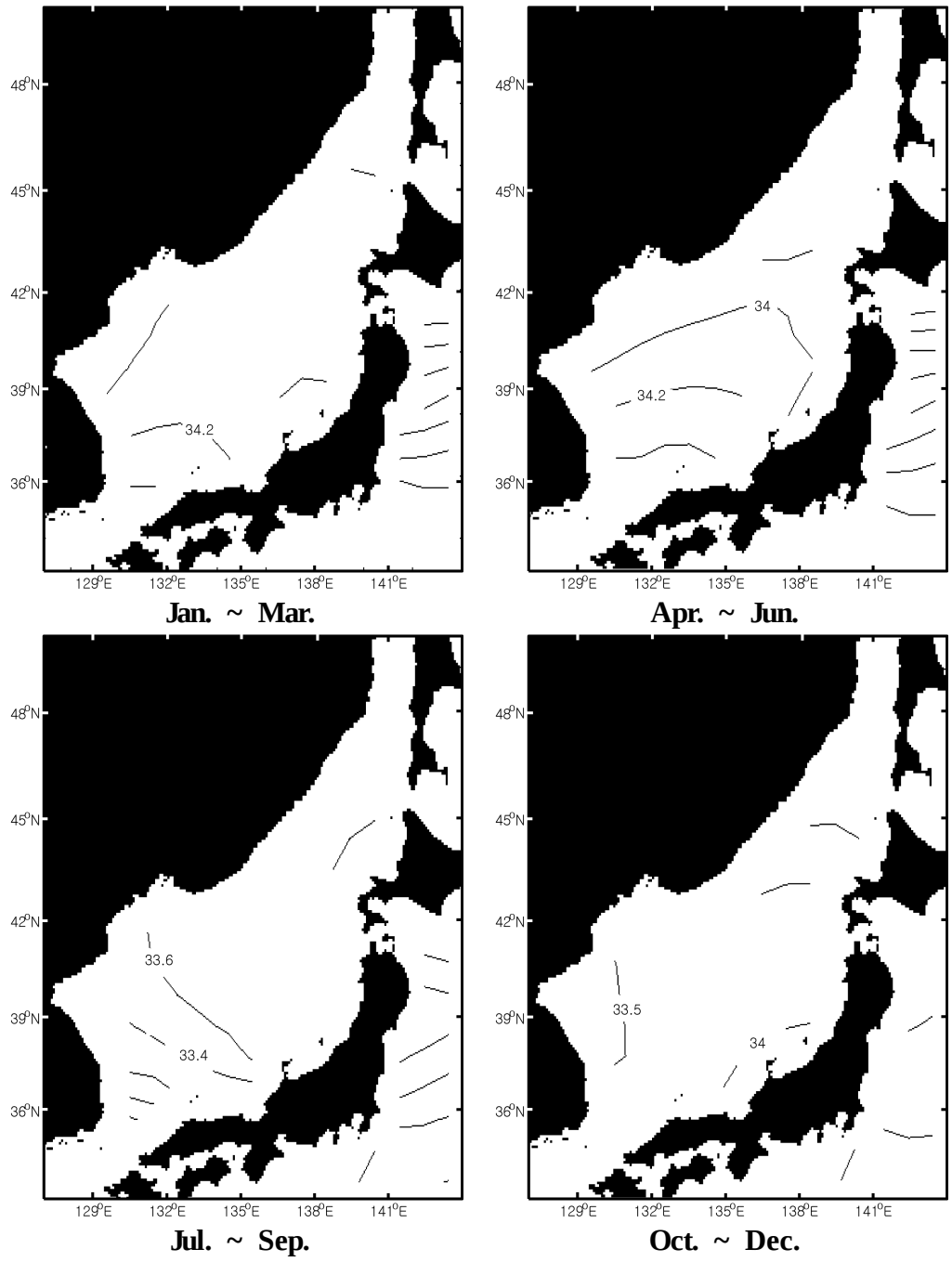

Fig. 4. Modern seasonal surface salinity distributions (‰) over in the East Sea. The SSS data were downloaded from the web site http://iridl.ldeo.columbia.edu/SOURCES/.NOAA/.NODC/.WOA98/.SEASONAL/.analyzed/.salinity/.

4. Material and method

The piston cores (05PC-14, 05PC-15, 05PC-23) were collected from the bathymetric high of the South Korea Plateau in 2005 by the R/V Tamhae Ⅱ of the Korea Institute of Geosciences and Mineral Resources (Fig. 5). Core 05PC-14 (3.77m long) was collected from upper continental slope of Donghae-Samcheok (129°42.86'E, 37°30.11'N) at 800m water depth. Core 05PC-15 (6.61m long) was obtained lower continental slope of Donghae-Samcheok (129°58.93'E, 37°33.16'N) at 1546m water depth. Core 05PC-23 (6.08m long) was taken from the flat top of Sokcho-Donghae Ridge (129°32.86'E, 38°24.14'N) at 1100m water depth. These coring sites are located beneath the northward flowing the TWC (Fig. 5). These piston core samples were analyzed for this study. These cores were divided from top to bottom into samples 1cm long, and all samples were used for alkenone analysis.

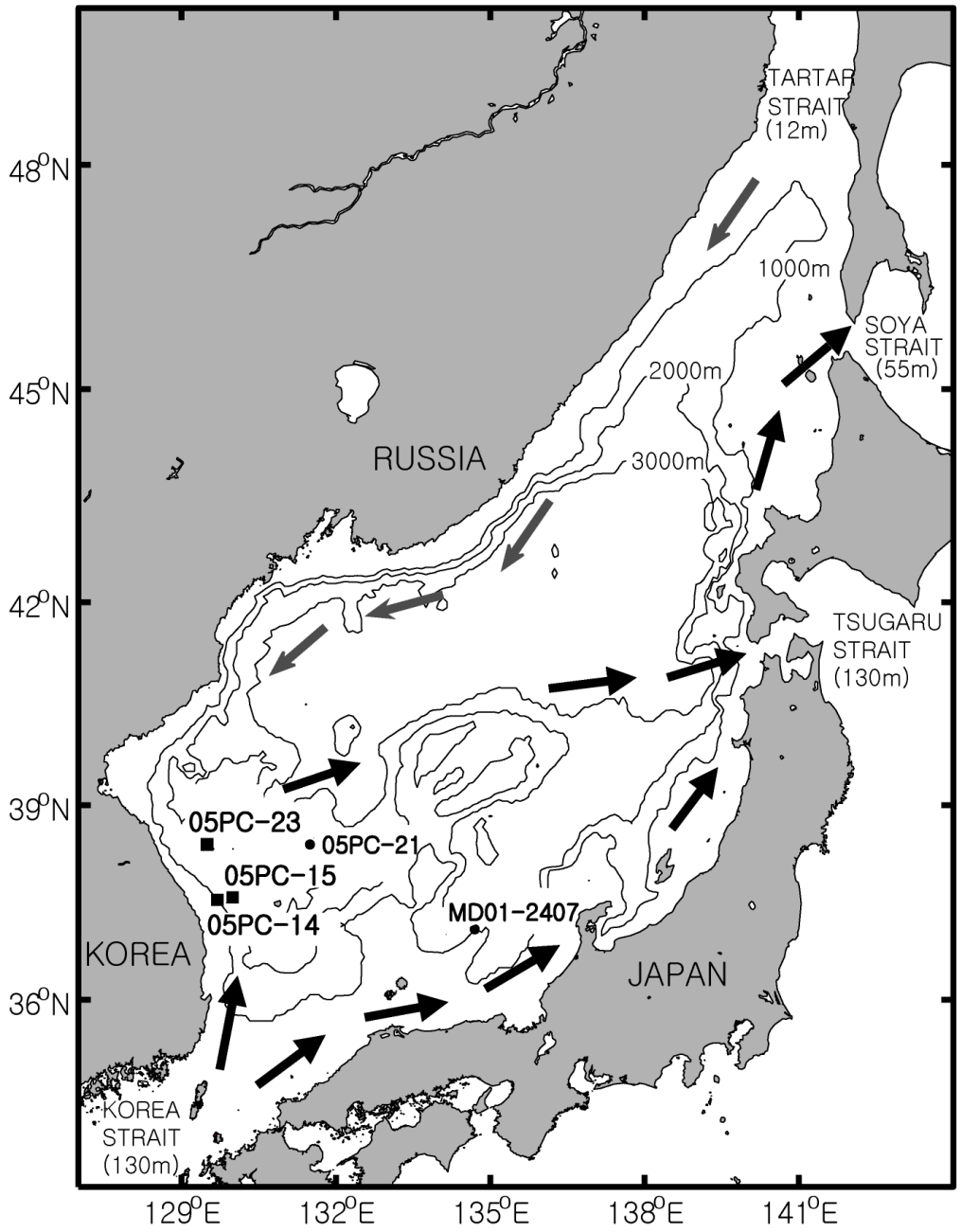

Fig. 5. Bathymetric map of the East Sea with three core locations (05PC-21, 05PC-23, and MD01-2407). Thick and thin arrows indicate the Tsushima Warm and Liman Cold Currents, respectively. Also shown is four major straits around the East Sea.

4-1. Alkenone analysis

Long-chain alkenones were extracted from surface sediments (about 1g) by ultrasonication using a HP 2070 with successively less polar mixtures of methanol and methylene chloride (MeOH ×1, MeOH/CH_2Cl_2 1:1 ×1, CH_2Cl_2 ×1) for 3min, respectively. After each extraction, the suspensions were centrifuged (using MF300 at 2000rpm for 5min) and the supernatants were combined. The combined extracts were washed with distilled water to remove sea salts and methanol, dried with preheated Na_2SO_4, and concentrated to near-dryness under N_2. The residues were redissolved in 100㎕ of CH_2Cl_2, and cleaned by elution with methylene chloride (500㎕ × 3) through a commercial silica cartridge (Bond Elut SPE column, 100mg/ml, #188-0110). Saponification was then performed at 70℃ for 2h with 0.1M KOH in Methanol. The alkenone fraction was obtained by partitioning into hexane. The final extracts were analyzed by capillary gas chromatography with a GC-17A gas chromatograph and Agilent 7890A equipped a 60m fused silica column (J&W DB-5MS, 0.32mm × 0.25㎛), and flame ionization detection. The GC oven was programmed from 60° to 200℃ at 20℃ min^{-1}, from 200° to 310℃ at 15℃ min^{-1}, and from 310° to 320℃ at 15℃ min^{-1}. The final temperature was maintained for 5min. The identification of compounds and verification of the absence of coelutions were performed by GC on selected samples. 2-nonadecanone,

Hexatriacontane, and n-Octatriacontane were used as the internal standard and the yield standard, respectively. One example of chromatograms resulting from the analysis of these diluted samples is shown in Fig. 6. We assumed that the flame ionization detector was equally sensitive to C_{37} alkenone and the internal standard. We calculated the alkenone unsaturation index as defined by Prahl and Wakeham (1987):

$$U^{K'}_{37} = [C_{37:2}] / ([C_{37:2}] + [C_{37:3}]) \quad [1]$$

where $C_{37:2}$ and $C_{37:3}$ represents the di- and triunsatured C_{37} alkenones, respectively (Prahl and Wakeham, 1987). Temperature estimates were based on the calibration of Prahl et al. (1988).

$$T = (U^{K'}_{37} - 0.039)/0.034 \quad [2]$$

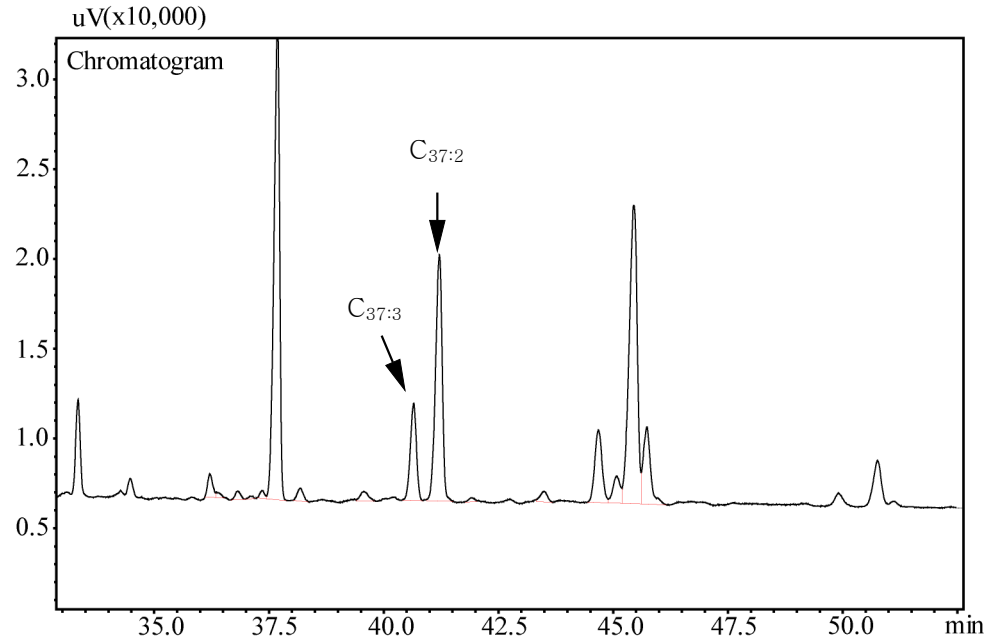

Fig. 6. Chromatograms of $C_{37:3}$ and $C_{37:2}$ extracted from sample 05PC-23 depth 14cm.

4-2. Age control

Datums including L* were provided from the Korea Institute of Geosciences and Mineral Resources (KIGAM). Lightness (L*) of the sediments was measured at 1cm interval on split core surface covered with a plastic wrap using spectrophotometer Minolta CM-2500d. The L* value is psychometric lightness and corresponds to black (L*=0) and white (L*=100).

The calendar age for this sediment was constructed using the correlation among 05PC-21, 05PC-23 and MD01-2407 (Fig. 6). The correlation among the three cores was based on the L* values and tephra layer (AT) supplement to the occurrence of the Thinly Lamination (TL) layer. 05PC-21 core was corrected at 1721m water depth on the Juksan Seamount (38°24.2'N, 131°32.8'E) during same cruise with 05PC-23. MD01-2407 (Kido et al., 2007) was corrected at 932m water depths on the Oki Ridge (37°04.0'N, 134°42.2'E) in the East Sea. The variation patterns of L* values among the three cores are similar. The peak and trough of distinct stage boundaries can be identified. In addition, the tephra layers are stratigraphic markers in the East Sea (Machida, 1999). The upper layer of TL-2 is identified at 40cm. Calendar age of TL-2 was measured from Accelerator Mass Spectrometry (AMS) ^{14}C dates for *G. bulloides* (size >212 um), and was identified 18.9 kyr. Aira-Tanzawa (AT) is identified at

90cm in the 05PC-23. Calendar age of the AT ash layer is identified at 29.4 kyr (Yokoyama et al., 2007). The TL-2 from 05PC-23 also complements the age and sedimentation rate. Continuous ages were estimated by linear interpolation assuming constant sediment rates between correlation layers. As a result, the age model shows that core 05PC-23 covers up to 130 kyr. Based on the L* values, cores 05PC-14, 05PC-15 were also correlated with core 05PC-23 (Fig. 7). The variation patterns of L* values between the three cores are very similar, from which the peak and trough of distinct stage boundaries can be identified. As a result, core 05PC-14 covers up to 78 kyr, and core 05PC-15 covers up to 110.7 kyr.

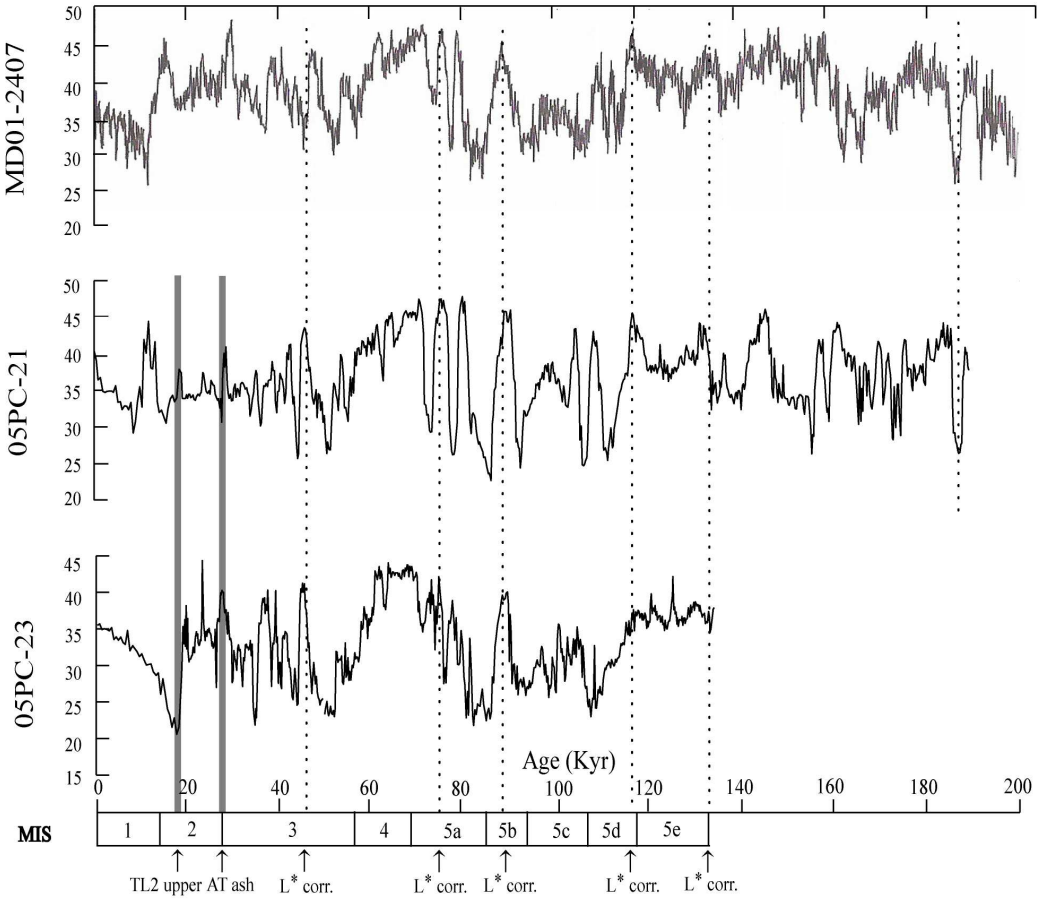

Fig. 7. Construction of age were constructed by correlation of L* values among the core MD01-2407 (Kido et al., 2007), 05PC-21, and 05PC-23.

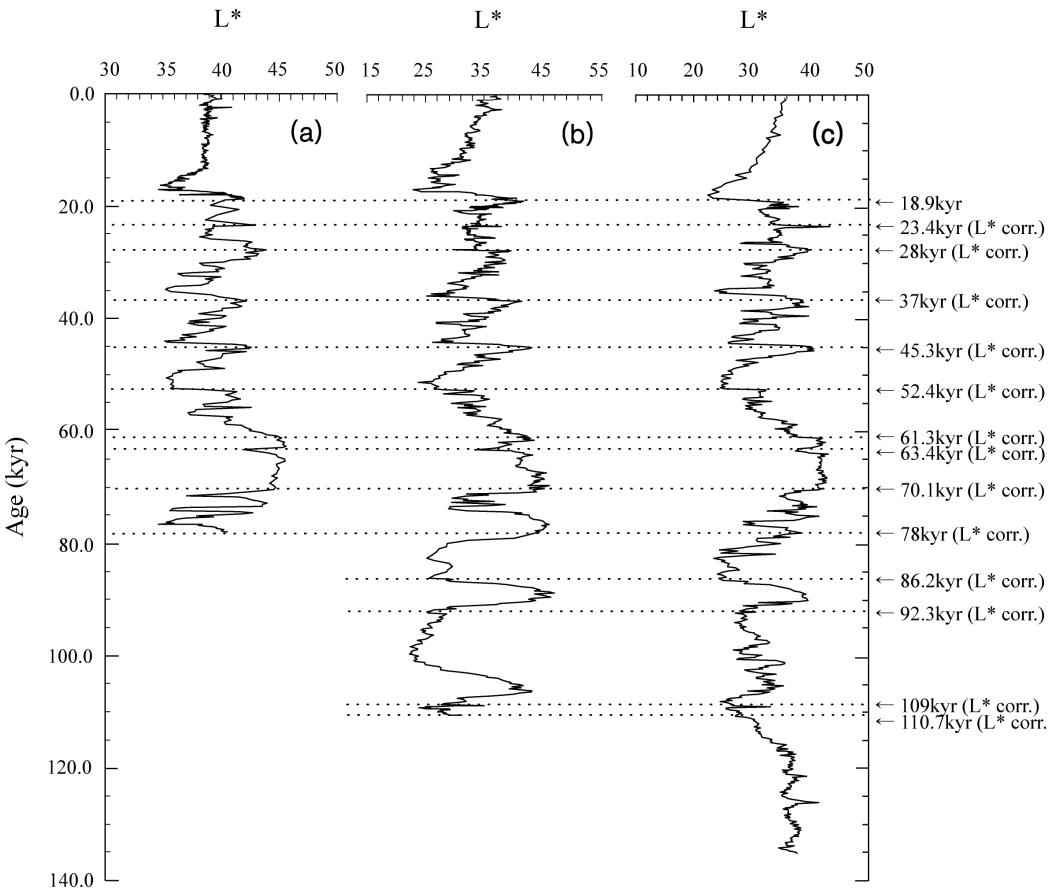

Fig. 8. Construction of age estimate by correlation of L* values of (a) core 05PC-14, (b) core 05PC-15 and (c) core 05PC-23.

5. Results

5-1. Calibration equation

In this study, the calibration equation of Prahl et al. (1988) was used to estimate the alkenone temperatures for all samples. Prahl et al. (1988) established the equation based on laboratory culture experiments of *E. huxleyi* collected from the northeastern Pacific. The alkenone unsaturation index, $U^{K'}_{37}$, is derived from the relative abundance of methyl alkenones with 37 carbon atoms and two or three double bonds ($U^{K'}_{37}$ = $[C_{37:2}]$ / ($[C_{37:2}]$ + $[C_{37:3}]$)). In our sediments, $C_{37:4}$ alkenone was found in relatively small quantities. For open ocean strain of *E. huxley*, $U^{K'}_{37}$ is better fit with the growth temperature than U^{K}_{37} (Prahl et al., 1988). Moreover, *E. huxleyi* is the main alkenone producer in the subarctic region of the North Pacific including the East Sea (Lee and Schneider., 2005). Therefore, Prahl's equation was the most appropriate equation for estimation SST in the East Sea.

5-2. 05PC-14

(1) Alkenone content

All of the alkenone analysis data measured from the 05PC-14 are

complied in Table 1 and Fig. 9. Variation of the content of total C_{37} alkenones over the 80 kyr BP is plotted in Fig. 9b. Sediments in core 05PC-14 contained very low contents of alkenones for the glacial period between 20.7 and 37.5 kyr BP (Fig. 9b). Therefore, the temperature estimated from the $U^{K'}_{37}$ values could not be estimated for the early MIS 2 between 20.7 and 29 kyr BP, and late MIS 3 between 29 and 37.5 kyr BP. During the MIS 5a, the contents is high, up to 8.4μg/g. Then, it decreases and fluctuates mainly between 0.1 and 0.5μg/g during MISs 3 and 4. However, alkenone contents rapidly increases up to 3.3μg/g at 50.98 kyr BP. After that, it ranges from 0.9 to 4.7μg/g during MIS 1. The mean values of the alkenone contents was 2.3μg/g in MIS 1, 1.2μg/g in early MIS 2, 0.5μg/g in MISs 3 and 4, and 3.7μg/g in MIS 5a. It results shows that abnormally high contents of alkenones occur during the MIS 5a and low contents of alkenones occur during the MISs 3 and 4.

(2) Alkenone temperature

The core top $U^{K'}_{37}$-derived temperature was 18.1℃. This estimated temperature is consistent with the monthly averaged temperature from the surface to 100m depth at a location close to 05PC-14 (NFRDI climatological database; Fig. 10). The alkenone temperature at the core top is close to temperatures in the upper 0m of the water column in May-Jun.

Variation in $U^{K'}_{37}$ temperature over the past 78 kyr in 05PC-14 is shown in Fig. 9a. The alkenone-based temperature decreased from 16.6℃ to 12.8℃ during the MIS 5a between 71.5 and 76.2 kyr BP. During the MIS 4 between 59.4 and 68.8 kyr BP, the low temperatures remained between 10.6℃ and 12.7℃. The temperature for the MIS 3 between 37.5 and 54.6 kyr BP fluctuated between 8.5℃ and 15.7℃. Alkenone SST increased rapidly up to 14.1℃ at 52 kyr BP, and then decreased up to 8.5℃ during the period of 44.9-52 kyr BP. During the 41.4-44.9 kyr BP, it remained between 9.5℃ and 10.5℃, and then increased slightly up to 15.7℃ during the period of 40.7-41.4 kyr BP. Finally, it rapidly decreased to 10.8 at 37.5 to 38.8 kyr BP. Due to the low content of alkenones, $U^{K'}_{37}$ values could not be calculated during early MIS 2 between 20.7 and 26.5 kyr BP and late MIS 3 between 27.2 and 37.5 kyr BP. During the early MIS 2 between 26.5 and 27.2 kyr BP, SST increased from 15.5 ℃ to 17.8℃. And during he late MIS 2 between 15.4 and 20.7 kyr BP, it varied from 13.8℃ to 16.0℃. During the early MIS 2 between 26.5 and 27.2 kyr BP and during the late MIS 2 between 15.4 and 20.7 kyr BP, SST were close to those of MIS 1.

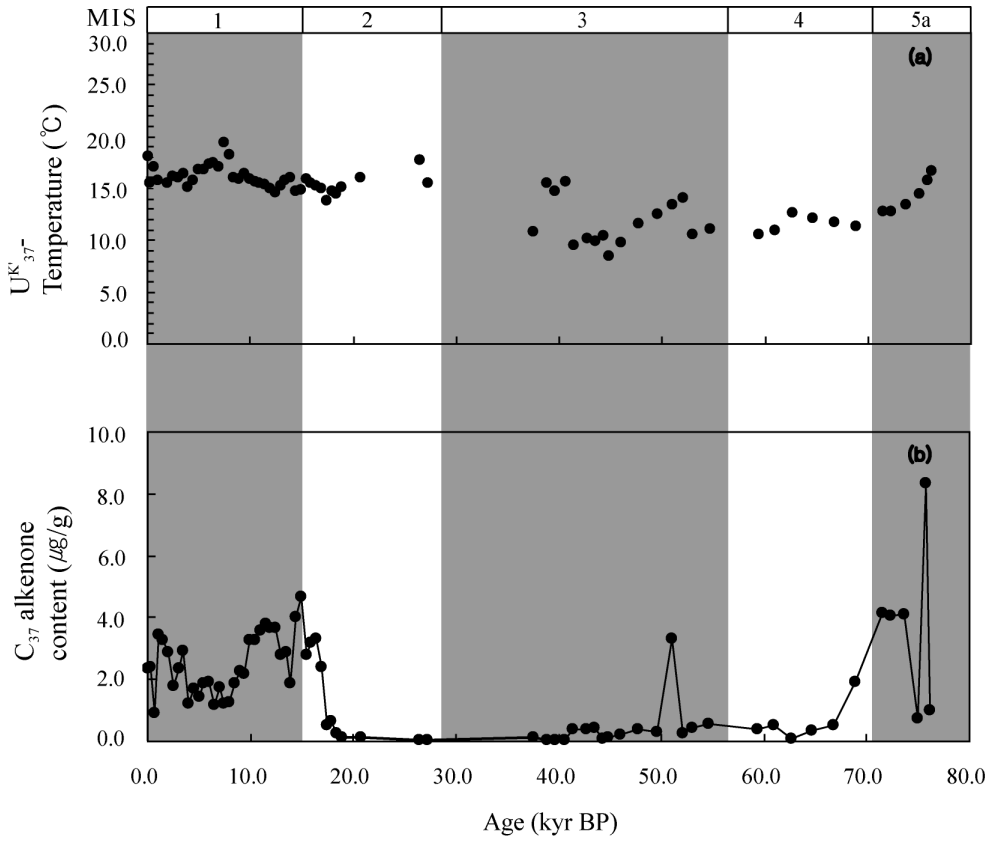

Fig. 9. (a) Alkenone-based SST estimates versus ages in core 05PC-14. (b) Total C_{37} alkenone content versus ages in core 05PC-14.

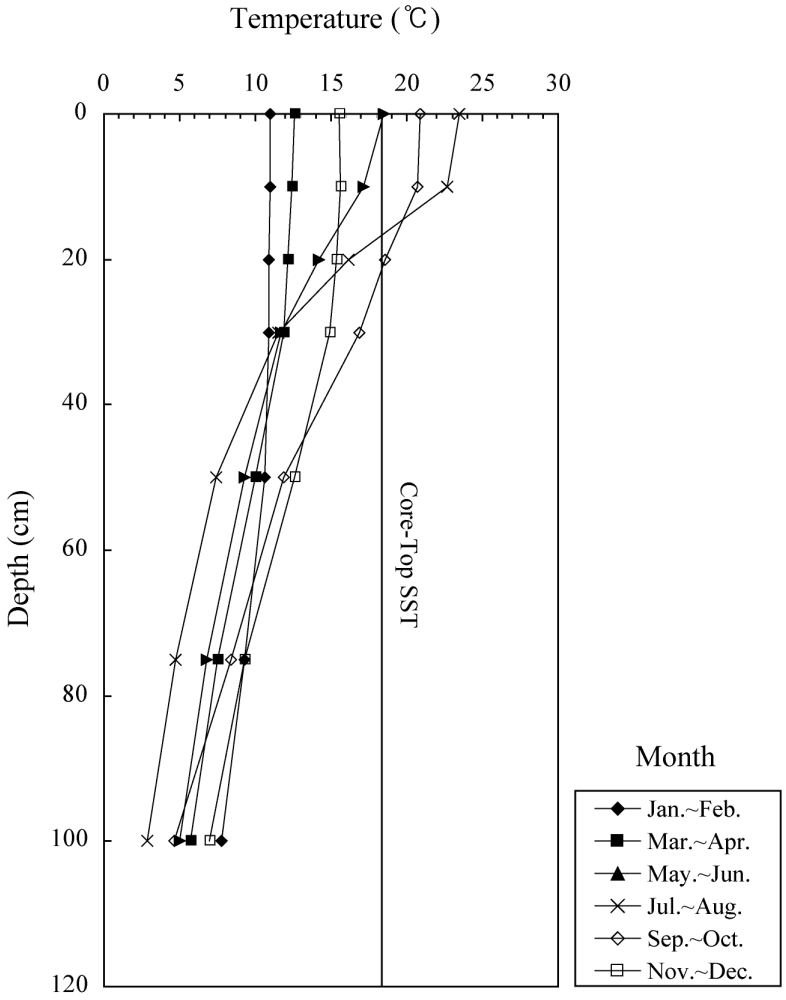

Fig. 10. Seasonal variations in the monthly averaged temperature from the surface to 100m depth at 37°332′N, 129°413′, near the core site of 05PC-14. The line at 18.1℃ represents the alkenone temperature at the core top.

5-3. 05PC-15

(1) Alkenone content

All of the alkenone analysis data measured from the 05PC-15 are compiled in Table 2 and Fig. 10. Variation of the contents of total C_{37} alkenones over the 110 kyr BP is plotted in Fig. 10b. Sediment in core 05PC-15 contained very low contents of long chain alkenones for the glacial period between 17.76 and 30.57 kyr BP (Fig. 11b). Therefore, the alkenone temperature estimated from the $U^{K'}_{37}$ values could not be estimated for the early MIS 2. In general, the content is relatively high during interglacial periods and low during glacial periods. During MIS 5, the contents is high, up to 2.7μg/g. Then, it decreases and ranges usually from 0.1 to 0.2μg/g during MISs 3 and 4. Anomalously, it increased rapidly up to 1.2μg/g at 51.32 kyr BP. After that, it ranges from 0.3 to 1.3μg/g during MIS 1. The mean values of the alkenone contents are 0.3μg/g in MIS 1, 0.5μg/g in MIS 2, 0.1μg/g in MISs 3 and 4, and 0.7μg/g in MIS 5. It results shows that abnormally high contents of alkenones occur during the MIS 5 and low contents of alkenones occur during the MISs 3 and 4.

(2) Alkenone temperature

The core top $U^{K'}_{37}$-derived temperature was 18.2℃. This estimated temperature is consistent with the monthly averaged temperature from the surface to 100m depth at a location close to 05PC-15 (NFRDI climatological database; Fig. 12). The alkenone temperature at the core top is close to temperatures in the upper 10m of the water column in May-Jun. Variation in $U^{K'}_{37}$ temperature over the past 110 kyr in 05PC-15 is shown in Fig. 11a. It ranged from 6.3℃ to 27.4℃, with highest value (27.4℃) occurring at 51.32 kyr BP and the lowest value (6.3℃) occurring at 30.57 kyr BP. The alkenone-based temperature fluctuated mainly between 14.1℃ to 23.3℃ during the period 86.2-109.38 kyr BP. During the period 66.45-86.2 kyr BP, the temperature decreased from 15.8℃ to 12.4℃. It increased from 12.4℃ to 19℃ during the period 63.40-66.45 kyr BP, and then it decreased up to 13.7℃ at 61.4 kyr BP. After that, it increased up to 27.4℃ at 51.32 kyr BP, and then it fluctuated between 15.1℃ and 27.4℃ during the period 33.33-51.32 kyr BP. During the period 30.57-33.33 kyr BP, the temperature rapidly decreased up to 6.3℃. It increased from 13℃ to 25.4℃ during the period 16.63-17.76 kyr BP, and then it decreased from 25.4℃ to 15.1℃ during the period 12.79-16.63 kyr BP. Thereafter, it continued to fluctuated between 15.1℃ and 18.2℃.

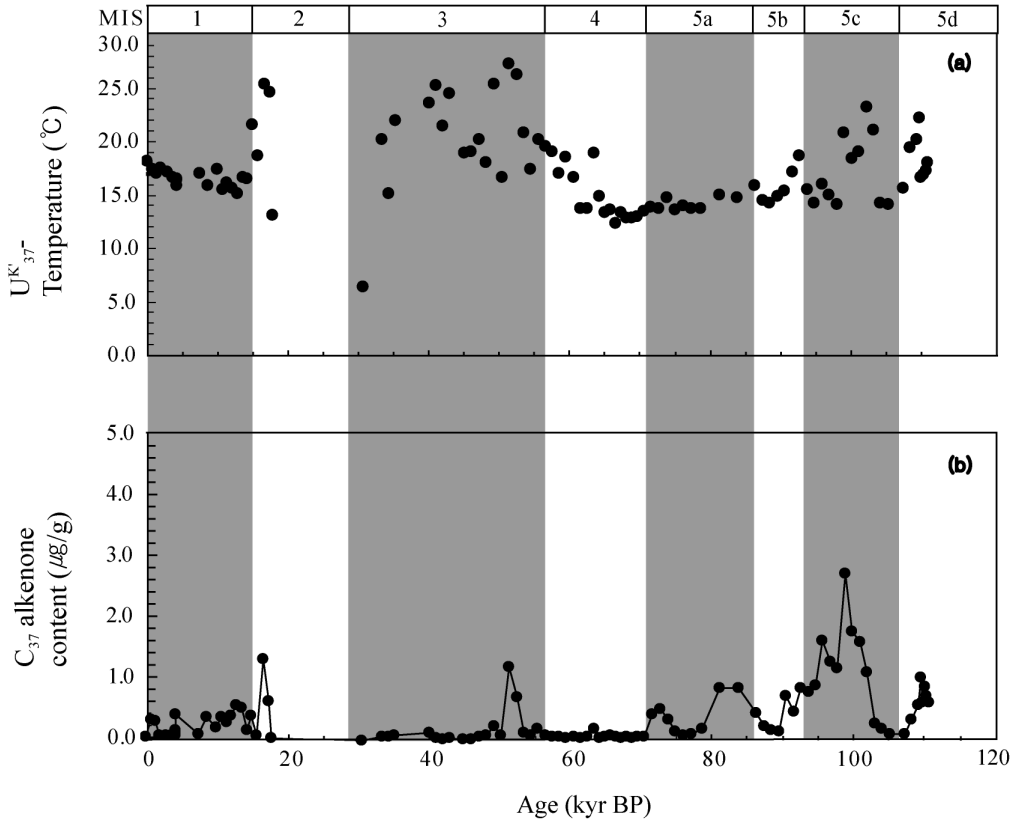

Fig. 11. (a) Alkenone-based SST estimates versus ages in core 05PC-15. (b) Total C_{37} alkenone content versus ages in core 05PC-15.

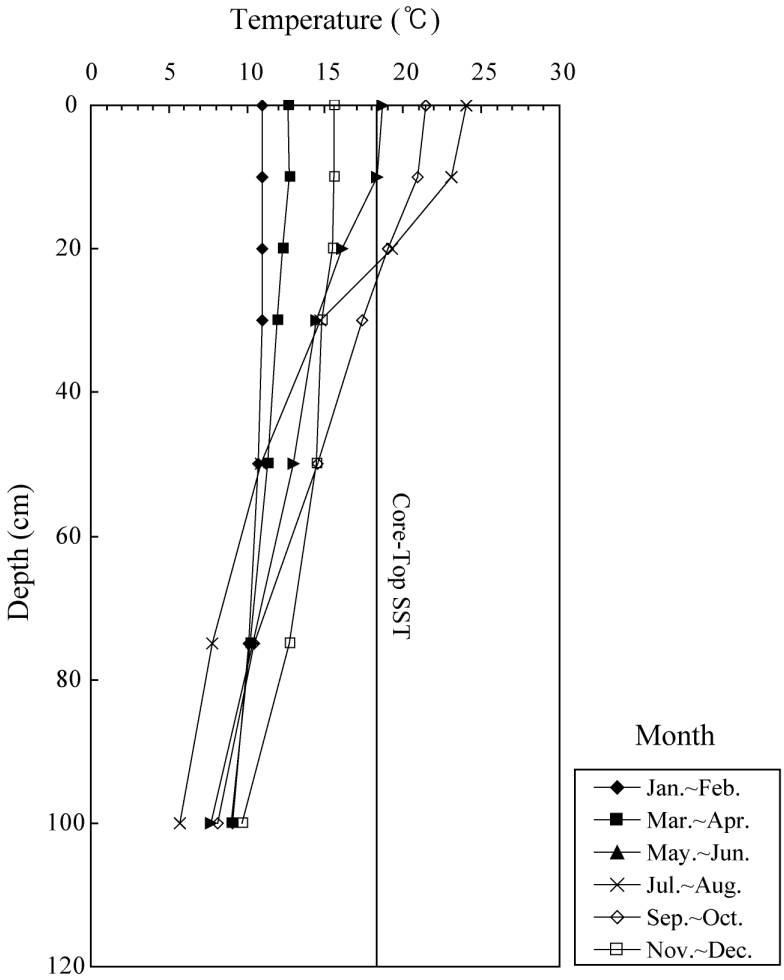

Fig. 12. Seasonal variations in the monthly averaged temperature from the surface to 100m depth at 37°332′N, 130°E, near the core site of 05PC-15. The line at 18.2℃ represents the alkenone temperature at the core top.

5-4. 05PC-23

(1) Alkenone content

All of the alkenone analysis data measured from the 05PC-23 are compiled in Table 3 and Fig. 11. Variation of the content of total C_{37} alkenones over the 130 kyr BP is plotted in Fig. 13b. Sediments in core 05PC-23 contain very low contents of long chain alkenones for the glacial period between 20.18 and 29.38 kyr BP (Fig. 11b). Therefore, the temperature estimated from the $U^{K'}_{37}$ values could not be estimated for early MIS 2. However, enough total C_{37} alkenone contents are available to be analyzed in sediments for the MISs 1, 3, 4, 5 and late MIS 2. During MIS 5, the contents high, up to 19.7μg/g. Then, it decreases and fluctuates between 0.1 and 2.9μg/g during MISs 3 and 4. In the same as core 05PC-14 and 05PC-15, it increased rapidly up to 5.5μg/g at 46.88 kyr BP. After that, it ranges from 0.1 to 3.2μg/g during MIS 1. Averaged alkenone contents for the MIS 5 is 3.76μg/g at MIS 5a, 2.36μg/g at MIS 5b, 3.3μg/g at MIS 5c, 4.3μg/g at MIS 5d and 2.62μg/g at MIS 5e. On the other hands, mean values of alkenone contents are 0.97μg/g in MIS 1, 1.3μg/g in late MIS 2, and 0.7μg/g in MISs 3 and 4. It results shows that abnormally high content of alkenone occurs during the MIS 5d and low content of alkenone occurs during the MIS 4.

(2) Alkenone temperature

The core top $U^{K'}_{37}$-derived temperature was 16.3℃. This estimated temperature is consistent with the monthly averaged temperature from the surface to 100m depth at a location close to 05PC-23 (NFRDI climatological database; Fig. 14). The alkenone temperature at the core top is close to temperatures in the upper 30m of the water column in Sep-Oct. Variation in $U^{K'}_{37}$ temperature over the past 130 kyr in 05PC-23 is shown in Fig. 13a. It ranged from 9.6℃ to 25.8℃, with highest value 25.8℃ occurring at 46.88 kyr BP and the lowest value 9.6℃ at 62.37 kyr BP. During the MIS 5e, the alkenone temperatures were high up to 18.2℃. During the MIS 5d, it decreased to 16.1℃, and then increased to 18.1℃ during the MIS 5c. During the MIS 5a and b, it dropped to 10.2℃. During the MIS 5e, the alkenone temperatures were higher than those of MIS 1.the MISs 5c and d, the temperatures were close to those of MIS 1. And during the MISs 5a and b, the temperatures were low. Alkenone-based SST decreased slightly during the MIS 4. The temperature for MIS 4 between 61.96 and 70.52 kyr BP fluctuated between 9.6℃ and 12.3℃. However, during the MIS 3 between 29.38 and 56.66, it was scattered between 13.5℃ and 25.8℃, and SST was abnormally warmer than Holocene despite of glacial period. The SST for Holocene period between 0 and 15.29 kyr BP varied from 15.7℃ to 17.4℃.

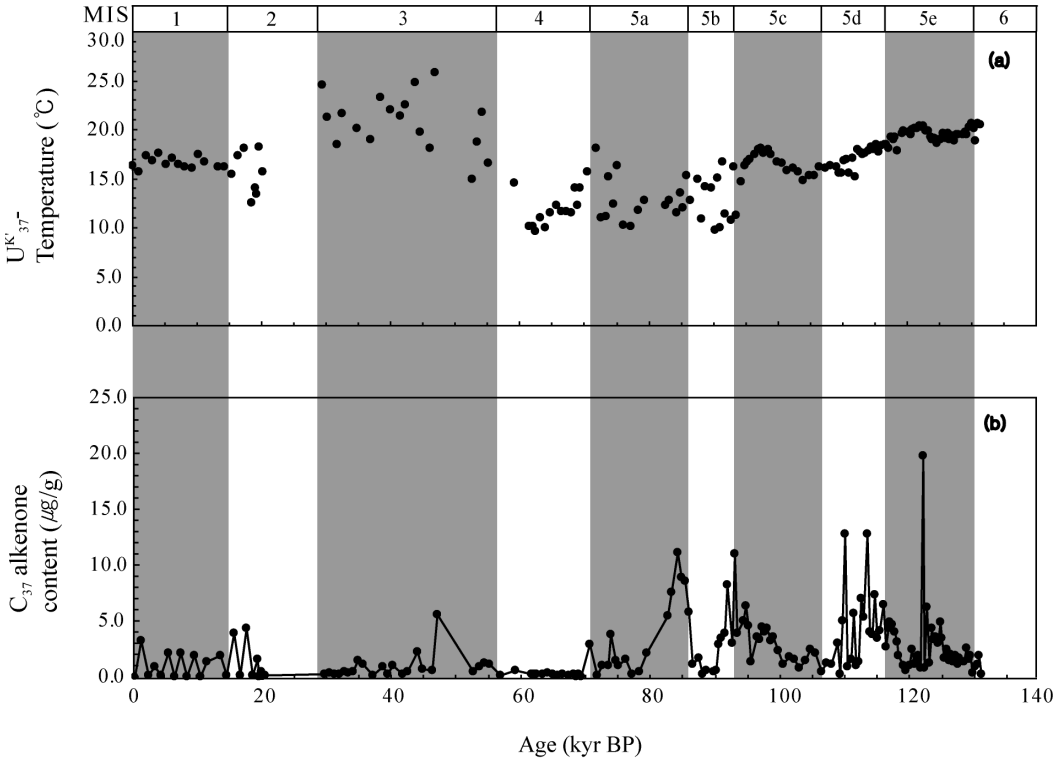

Fig. 13. (a) Alkenone-based SST estimates versus ages in core 05PC-23. (b) Total C_{37} alkenone content versus ages in core 05PC-23.

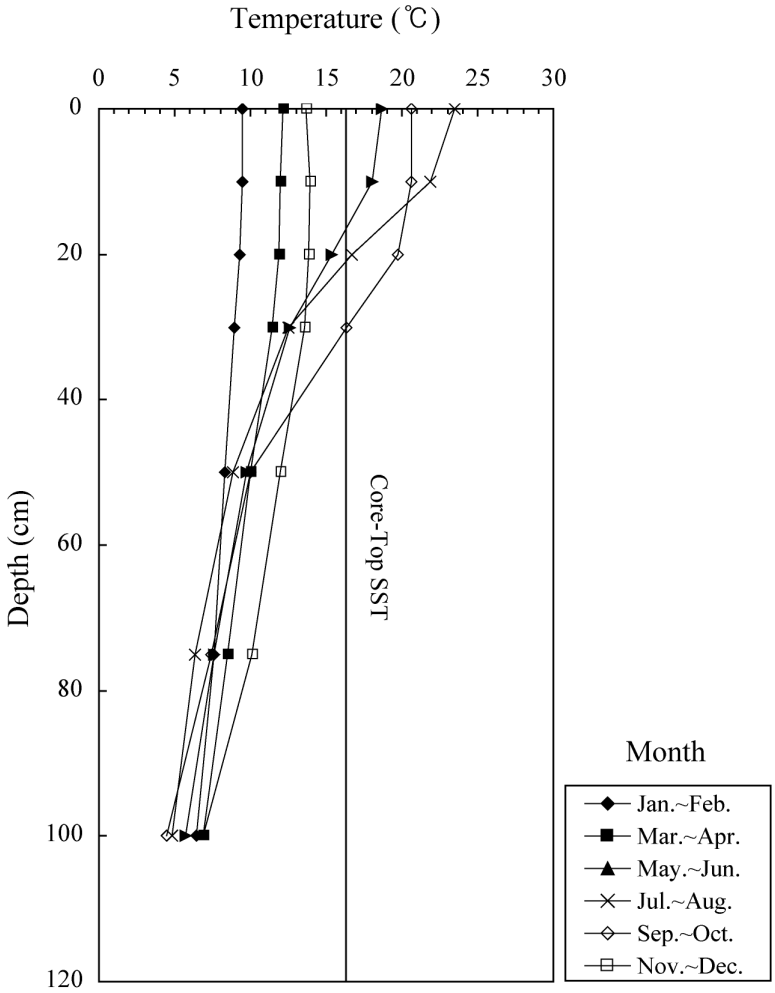

Fig. 14. Seasonal variations in the monthly averaged temperature from the surface to 100m depth at 38°126′N, 129°411′E, near the core site of 05PC-23. The line at 16.3℃ represents the alkenone temperature at the core top.

6. Discussion

6-1. Analytical error of GC

In order to confirm analytical error of GC, chromatograms of 05PC-14, 05PC-15 and 05PC-23 were compared. We used two types of gas chromatograph. The samples of 05PC-14 and 05PC-23 were analyzed by capillary gas chromatography with Shimadzu GC-17A gas chromatograph, and the samples of 05PC-15 were analyzed by capillary gas chromatography with Agilent 7890A gas chromatograph. We used one types of fussed-silica columns, HP-5MS ((5%-phenyl)-methyl polysiloxane; length, 60m; inner diameter, 0.32 mm). We compared the difference of chromatograms among the 05PC-14 (depth 300cm, 53 kyr BP), 05PC-15 (depth 375, 52.4 kyr BP) and 05PC-23 (depth 230, 53 kyr BP). A representative chromatograms of the C_{37} alkenone composition is shown in Fig. 15. The identification of compounds was performed using the internal standard (I.S.; n-Octatriacontane). For the chromatogram of 05PC-14, alkenones and alkenoates typically elute between 33 and 38min and the $C_{37:3}$ and the $C_{37:2}$ are well separated. The alkenone temperature was calculated as 10.6℃ (Fig. 15a), which is the reliable values for this core sample (05PC-14). For the chromatogram of 05PC-15, alkenones and alkenoates typically elute between 33 and 39min, the alkenone temperature was calculated as 26.4℃ (Fig. 15b), which is quitely higher than those of depth 300cm in 05PC-14 (Fig. 15a). For the chromatogram of 05PC-23,

alkenones and alkenoates typically elute between 43 and 55min, the alkenone temperature was calculated as 18.7℃ (Fig. 15c), which is also higher than those of depth 300cm in 05PC-14 (Fig. 15a). In chromatograms of each core, there are 2 large peaks (≥5000μV, ≥10 pA) and 2-3 small peaks (<5000μV, <10pA) between C_{37} alkenones and I.S. peaks, and C_{38} components after 3-5min from C_{37} alkenones. Though different in retention time, the chromatograms among the each core were similar in pattern of alkenones and alkenoates. It shows that chromatograms of each core, 05PC-14, 05PC-15 and 05PC-23, is reliable.

Alkenone contents in core 05PC-15 were very low, which is especially about 5 times lower than those of other two cores (Fig. 16). In order to find out the reason of significant low alkenone contents of 05PC-15, difference of the alkenone contents between Agilent 7890A and Shimadzu GC-17A was confirmed using 5 samples obtained from 05PC-23, which are 108, 128, 156, 184, 248cm. For the Agilent 7890A, the alkenone contents were calculated as 0.03-0.22μg/g (Fig. 17). On the other hand, for the Shimadzu GC-17A, the alkenone contents were calculated as 0.16-2.22μg/g (Fig. 17). Although the contents of same samples in 05PC-23, the alkenone contents obtained with the Agilent 7890A was slightly smaller than that obtained with the Shimadzu GC-17A. Therefore, relatively low contents of 05PC-15 is caused by different, which Agilent 7890A and Shimadzu GC-17A.

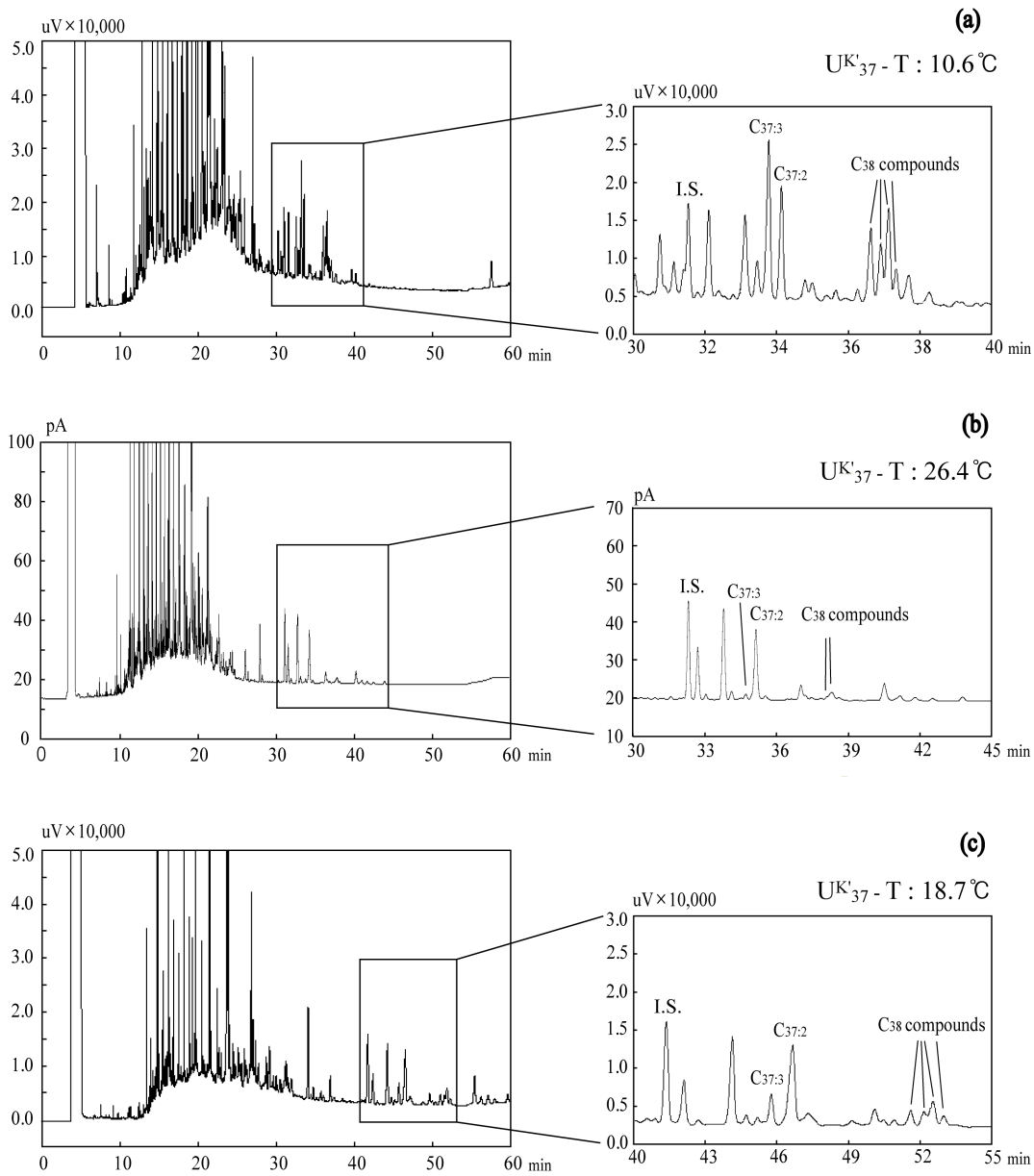

Fig. 15. Representative gas chromatograms of sedimentary samples containing mixtures of long-chain ketones and alkenones on analysis with (a) depth 300cm (53 kyr BP) of 05PC-14, (b) depth 375cm (52.4 kyr BP) of 05PC-15 and (c) depth 232cm (53.4 kyr BP) of 05PC-23. $C_{37:3}$: heptatriaconta (8E,15E,22E)-trien-2-one, $C_{37:2}$: heptatriaconta-(15E,22E)-dien -2-one, I.S. Internal Standard (n-Octatriacontane).

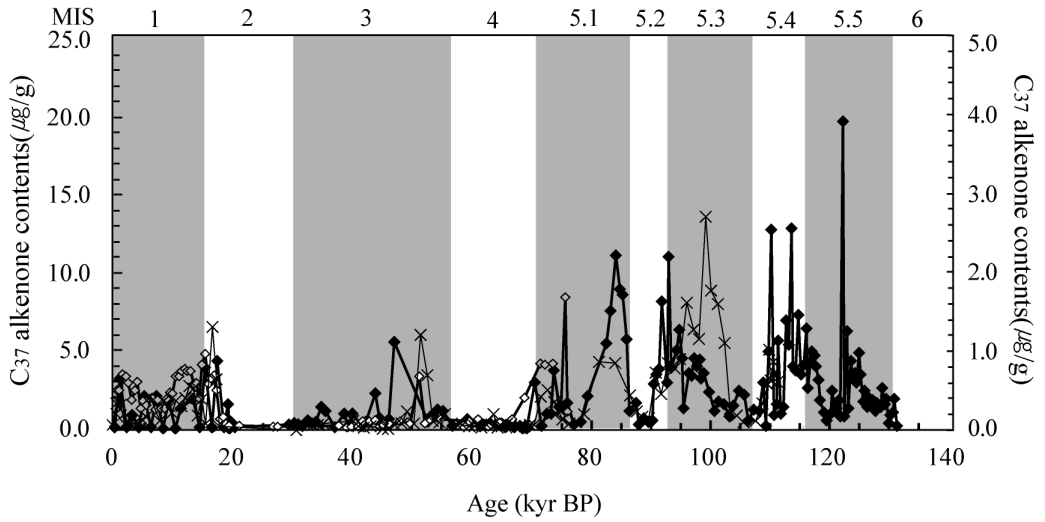

Fig. 16. Comparison of alkenone contents among the 05PC-14(◇), 05PC-15(×) and 05PC-23(◆). The left axis is of 05PC-14 and 05PC-23, the right axis is of 05PC-15.

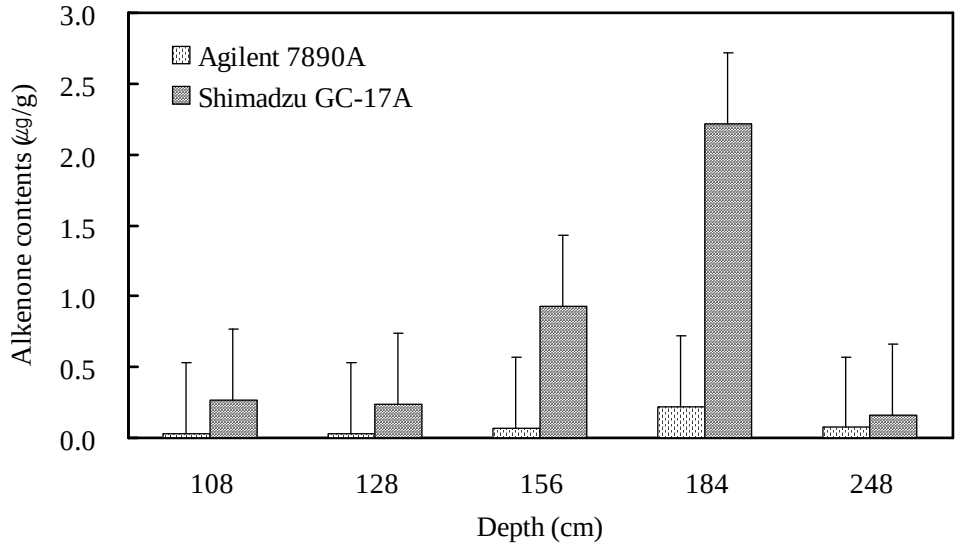

Fig. 17. Comparison of alkenone contents between Agilent 7890A and Shimadzu GC-17A.

6-2. Variation in sea surface temperature

Alkenone temperatures in the East Sea have largely fluctuated in accordance with global climate record during the late 130 kyr. Variation in alkenone temperatures of 05PC-14, 05PC-15, 05PC-23 is compared each other (Fig. 18). During the period of MIS 1- MIS 5, variation of the alkenone temperature in the East Sea is discussed in detail below.

(1) MIS 5

The change of the SST during the MIS 5 was shown in 05PC-14, 05PC-15 and 05PC-23. 05PC-14 covers up to MIS 5a, 05PC-15 covers up to MIS 5d, and 05PC-23 covers up to MIS 5e. For the 05PC-14, the alkenone temperature decreased from 16.6℃ to 12.6℃ during the MIS 5a. The average value of SST was 14.3℃ in MIS 5a. For the 05PC-15, the alkenone temperature decreased to 15.6℃ during the MIS 5d. During the MIS 5c, it increased slightly to 23.3℃, and then decreased to 14.2℃. During the MISs 5a and b, it dropped up to 13.8℃. The average values of alkenone temperature were 18.3℃ in MIS 5d, 17.2℃ in MIS 5c, 15.8℃ in MIS 5b, and 14.1℃ in MIS 5a. For the 05PC-23, the alkenone temperatures were high up to 18.2℃ during the MIS 5e. During the MIS 5d, it decreased to 16.1℃, and then increased to 18.1℃ during the MIS 5c. During the MISs 5a and b, it dropped up to 10.2℃. The average values of alkenone temperature were 19.5℃ in MIS 5e, 17.2℃ in MIS 5d, 16.3℃ in MIS 5c, 12.8℃ in MIS 5b, and 12.9℃ in MIS 5a. According to

results of these three core, very warm alkenone temperature events occurred during MIS 5e, which is higher than those of MIS 1. During the MISs 5c and d, alkenone temperature corresponded to the period of MIS 1. In particular, the temperatures of MISs 5a and b were lower than those of MIS 1.

The change of the East Sea SST is related to the atmosphere-ocean circulation regime of the Northern Hemisphere (Irino and Tada, 2002). Especially, temperature in the East Sea is chiefly controlled by the winter and summer monsoons. The cold, dry winter monsoon winds blow from the Asian continent and become wetter over the East Sea due to high evaporation from the TWC. On the other hand, the warm and moisture summer monsoon winds southwesterly blow and become increase of river discharge. Rather, the change of the SST in the East Sea seems to be related with air temperature changes which is consistent with changes in air temperature at high latitude. Zhang et al. (2002) studied atmospheric change using estimates of dust input to the Chinese Loess Plateau, which indicate millennial-scale variation in the winter monsoon climate. This study suggested that during the interglacial, Asian winter monsoons were weaker than those of the glacial. These could induce the surface warming of the East Sea during MIS 5c to 5e. However, alkenone temperatures for MISs 5a and b were lower than those of present. Ikehara et al. (2007) discussed the relationship between winter monsoon and summer monsoon fluctuations for MIS 5 using record of dark-colored layers. The dark layers represent strong summer monsoons and/or weak winter monsoon, and the light layers

represent strong winter monsoons and/or weak summer monsoon (Tada et al., 1995; Tada et al., 1999; Wang and Oba, 1998). This study suggested that intensity of winter monsoon upwardly increased during MIS 5. Therefore, progressive cooling during MISs 5a and b might be influenced by strong winter monsoon and/or weak summer monsoon in the western margin of the East Sea. It could induce fall of the SST in the study area.

Global sea-level change also may have influenced to change the SST in the East Sea. In the case of the East Sea, fall of sea level could restrict the inflow of TWC into the East Sea, resulting in preventing supply of warm current into the East Sea. Fall of sea level was closely related to sea-ice volume expansion. Lambeck et al. (2002) suggested that during the MIS 5, the change of the maximum global sea level due to the expansion of ice volume was considered to be less than 60m. Due to a global sea-level fall of 60m, the straits were most likely narrower than those of present, resulting in restricting the inflow to and outflow from the East Sea. According to study of Tada et al. (1999), as the fall sea levels of 60m, mode of ocean circulation in the East Sea is 3rd mode of four different modes. The third mode corresponds to periods with intermediate sea levels (-60 ~ -20m) when influx across the sills become significant and the relative contributions of the TWC and ECSCW varied significantly. Therefore, most of the alkenone components would be made when a strong influx of ECSCW would have supplied enough nutrients to sustain high surface productivity. Temperature of ECSCW is relatively lower than those of TWC. As a result, strong inflow of ECSCW into the East Sea could

induce the surface cooling during MISs 5a and b. Change of Asian monsoon system and change of inflow to the East Sea played an important role for the change of the alkenone temperature in the East Sea during the MIS 5.

(2) MISs 3 and 4

During the MIS 4, alkenone temperatures in 05PC-14, 05PC-15 and 05PC-23 were low up to 8.5℃, 12.4℃ and 9.6℃, respectively. The ice volume equivalent sea level was approximately 60-80m below at that time (Waelbroeck et al., 2002). The change of inflow into the East Sea could affect the SST in study area. In addition, strong winter monsoon could cool down the surface waters during the glacial period (Wang et al., 2005).

The $U^{K'}_{37}$-derived temperatures were relatively low in MIS 4 up to the middle of MIS 3, whereas they were relatively high in middle MIS 3 up to late MIS 3. During the middle MIS 3, alkenone temperatures in 05PC-14, 05PC-15, and 05PC-23 were high up to 14.1℃ , 27.4℃ , and 25.7℃, respectively. Among the results of palaeoceanographic studies, SST of MIS 3 in the East Sea is uncertain. Fujine et al. (2006) indicated that $U^{K'}_{37}$-derived temperatures were relatively high in middle MIS 3 up to late MIS 3 in the East Sea. However, considering a global sea level fall of 60-80m (Waelbroeck et al., 2002) and strong winter monsoon (Wang et al., 2005) during the last glaciation, warm alkenone temperature during the MIS 3 would be anomalous. However, the characteristic thing in our cores is

that core depth including abruptly high alkenone temperature in middle MIS 3 was showed Dark Laminate Muds (DLM), which occurred in 290-299cm of 05PC-14, 364-370cm of 05PC-15, and 210-228cm of 05PC-23 (Fig. 19). Also, according to sedimentary facies analysis of these cores, core depth including DLM coincided with those of abrupt high alkenone contents (0.3μg/g to 3.3μg/g in 05PC-14, 0.1μg/g to 1.2μg/g in 05PC-15, and 0.4μg/g to 5.5μg/g in 05PC-23). DLM was caused by bottom-water anoxic condition owing to water-column stratification (Demasion and Moore., 1980). Tada et al. (1999) studied that the bottom water oxygenation level was estimated on the basis of the S_{pyrite} versus C_{org} relationship in conjunction with the presence or absence of parallel laminations. C_{org} versus S_{pyrite} plots, as well as S_{pyrite}/C_{org} ratios, are commonly used to differentiate euxinic from non-euxinic bottom waters (Leventhal, 1983; Berner and Raiswell, 1983). As a result, in their view, during the period of low sea level (-60 ~ -90m), deep water oxygenation fluctuated between anoxic and oxic conditions corresponding to increases and decreases in the relative contribution of ECSCW to the influx. Since the influx through the Tsushima Starit was still restricted during this period, leading to anoxic bottom water conditions and deposition of dark layers. It seems that anoxic bottom water condition influenced abrupt high alkenone contents during the MIS 3, but it is insufficient that why alkenone temperature abruptly increase during the MIS 3. Therefore, further research is necessary to understand abruptly warm alkenone temperature during the glaciation period. It will be concluded in next chapter 6-3.

(3) MIS 2

During early MIS 2 between 20 and 30 kyr BP, the alkenone contents were extremely low. Due to the low content of alkenone, $U^{K'}_{37}$ values could hardly be calculated for this period. This is general pattern of cores from the East Sea (see the results of Ishiwatari et al., 2001 and Lee et al., 2008). It seems that extremely low content of alkenone in this study area was caused because the inflow of TWC into the East Sea was restricted between 20 and 30 kyr BP (Oba et al., 1991; Gorbarenko and Southon, 2000). It's because the TWC plays an important role in controlling the distribution of *E. huxleyi*, which would be the major source of alkenone even during the glacial period (Ishiwatari et al., 2001). Therefore, low alkenone contents may reflect the restricted inflow of the TWC. Oba et al. (1991) suggested that a global sea-level fall of 120m during the last glaciation would have restricted the inflow of TWC into the East Sea. Gorbarenko and Southon. (2000) also supported the hypothesis that TWC didn't flow into the East Sea at this time. Ryu et al. (2005) studied the diatom floral record taken from the southwestern margin of the Ulleung Basin in order to define the change in sea level during the late Pleistocene-Holocene. This study suggested that the sea level was low enough to close the shallow sills of the East Sea during the last glacial maximum (LGM). These studies stand with our result. Therefore, during this period between 20 and 30 kyr BP, restricted inflow of TWC into the East Sea could induce the low alkenone contents in the study area.

During the MIS 2, alkenone temperature in the East Sea is uncertain. Some alkenone temperatures from 15 to 20 kyr were anomalously high, even higher than those of the Holocene. In particular, high alkenone temperatures at this time have been reported previously for the East Sea (Fujine et al., 2006; Harada et al., 2006; Lee et al., 2008). Harada et al. (2006) supposed that these warm alkenone temperature episode would have had multiple causes, which are the shift of main season of alkenone production, sea-ice melting, and active Asian summer monsoon. Fujine et al. (2006) suggest that the warm SST was attributable to the physiological influence of low salinity on $U^{K'}_{37}$ values. However, Lee et al. (2008) discussed that low salinity conditions in MIS 2 would be expected to have happened in the East Sea. Rather, it's not clear for what to be a major factor responsible for the anomalously warm alkenone temperature. Further studies are necessary.

(4) MIS 1

The alkenone temperature increased up to the present temperature in the early MIS 1, it fluctuated between 15℃ and 18℃ (Fig. 20). Several studies suggested that the ice-volume equivalent sea-level rose to the present position at mid MIS 1 (8-10 kyr BP). According to proxy records of temperature and salinity in the East Sea, the warm and saline Tsushima Current flowed into the East Sea at this time (Oba et al., 1991; Jian et al., 2000; Lee, 2007). Considering the SST in core 05PC-14, 05PC-15 and

05PC-23 fluctuated between 15℃ and 18℃ throughout MIS 1, the East Sea was influenced by strong summer monsoon and/or weak winter monsoon during early MIS 1.

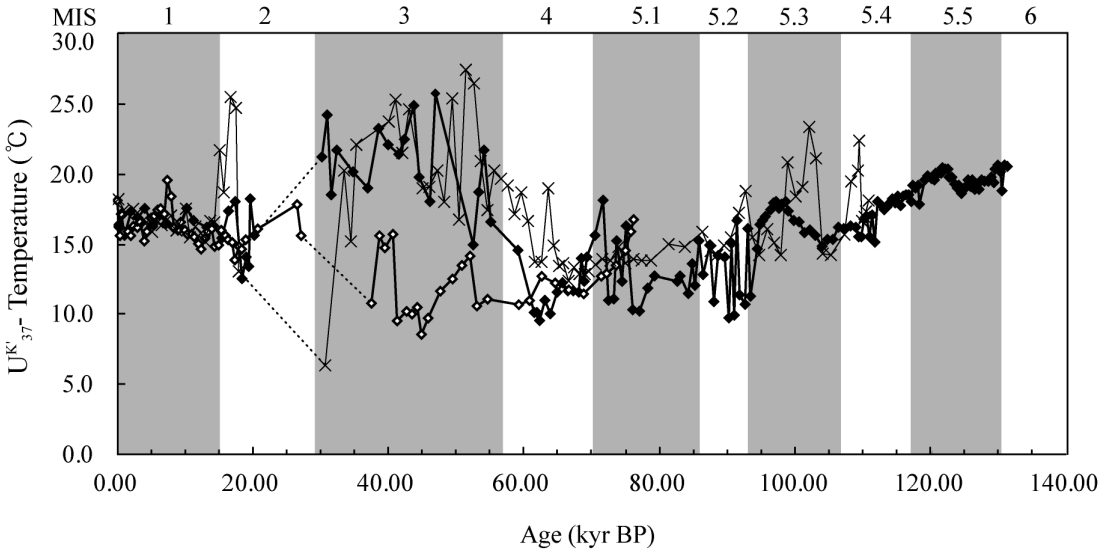

Fig. 18. Comparison of alkenone temperature change among 05PC-14(◇), 05PC-15(×), and 05PC-23(◆) during 130 kyr BP.

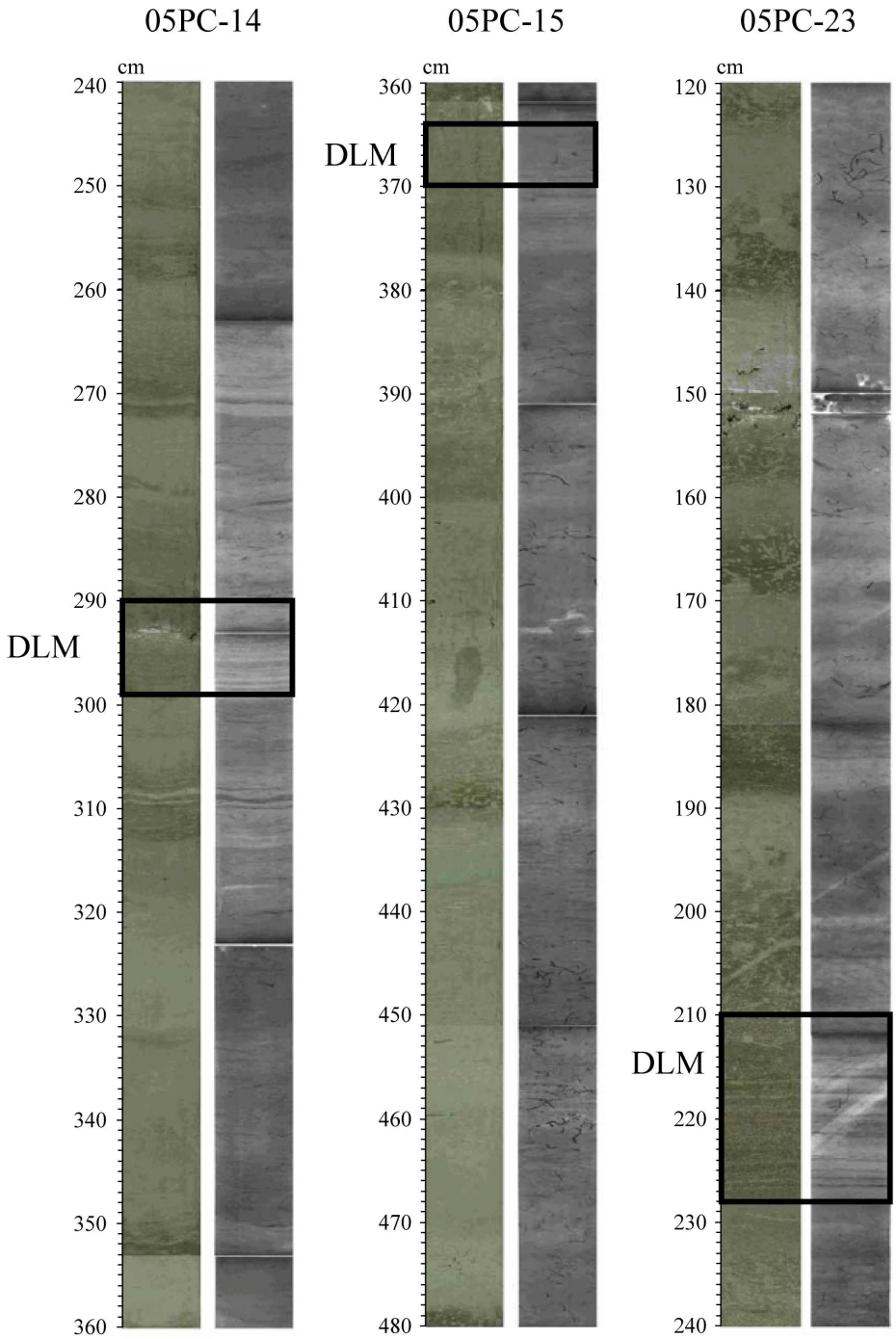

Fig. 19. DLM in Photographs and X-radiographs of core 05PC-14, 05PC-15, and 05PC-23 (KIGAM REPORT, 2004).

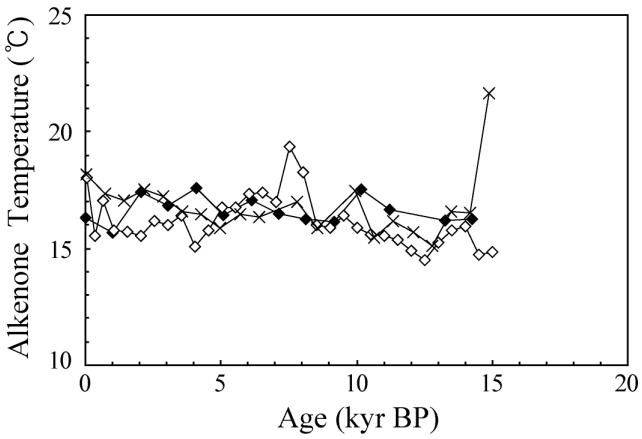

Fig 20. Comparison of alkenone temperature among 05PC-14(◇), 05PC-15(×), and 05PC-23(◆) during Holocene between 0-15 kyr.

6-3. Anomalously warm alkenone temperature during the glacial period

Warm alkenone temperature episodes occurred during 15-60 kyr BP, corresponding to the glacial period. Alkenone temperature fluctuated between 8.5℃ and 17.8℃ in 05PC-14, between 15.1℃ and 27.4℃ in 05PC-15, and between 14.9℃ and 25.7℃ in 05PC-23 (Fig. 21). Some possibilities were considered in order to explain the occurrence of such warm SSTs during the glacial period.

The first possibility is an effects of haptophyte species on alkenone-SSTs. Long-chain methyl ketones with two to four double bonds (alkenones) are biosynthesized by some algae of the class Haptophyceae / Prymnesiophyceae, such as *Emiliania huxleyi*. *E. huxleyi* is the most abundant and widespread coccolithophorid in the oceans and is most probably the main producer of alkenones found in recent sediments. However, species *G. oceanica*, which is closely related *E. huxleyi*, are known to synthesize C_{37}-C_{39} methyl and ethyl alkenones and related alkenoates (Marlowe et al., 1990; Volkman et al., 1995). According to a laboratory cultures of a single strain of *G. oceanica*, the difference in the $U^{K'}_{37}$ vs. SST relationship between the two species is controversial (Volkman et al., 1995). Recently, however, Conte et al. (1998) studied that selected warm and cold water strains of the coccolithophorid *E. huxleyi* and the *G. oceanica* were cultured under controlled temperature conditions to assess genetic and physiological variability in the alkenone/alkenoate vs. temperature relationship. Conte et al. (1998) argued that the $U^{K'}_{37}$ vs. SST

relationship for *G. oceanica* is different with those for cultured strains of *E. huxleyi*. Therefore, a difference of the linear equations expressing the $U^{K'}_{37}$ vs. SST relationship between the two species must be considered. Volkman et al. (1995) and Sawada et al. (1996) showed from laboratory cultured strains of *E. huxleyi* and *G. oceanica* that the SST estimated from *G. oceanica* being higher than that for *E. huxleyi* at the same $U^{K'}_{37}$ value; the difference of the SST values between the two species is 10.9℃ at 0.1 $U^{K'}_{37}$ value. Therefore, if the coccolith assemblages in the East Sea were dominated by *G. oceanica* over the glacial period, the $U^{K'}_{37}$ vs. SST relationship would be obtained for *G. oceanica,* and then SSTs obtained after correction for the presence of *G. oceanica* would be higher than the uncorrected SSTs.

The second possibility is a salinity effects on alkenone-SSTs. A number of the studies have revealed the influence of salinity on the $U^{K'}_{37}$ index (Sonzogni et al.l, 1997; Sikes et al., 1991; Rosell-Melé, 1998). Sonzogni et al. (1997) conducted the relationship between SST, salinity, and $U^{K'}_{37}$ index measured from the Bay of Bengal and the Arabian Sea, which is showed high salinity change between 31‰ and 36%. According Sonzogni et al. (1997), salinity change does not influence $U^{K'}_{37}$ index. Sikes et al. (1991) studied differences between core-top $U^{K'}_{37}$ temperatures and overlying SST caused by low salinity in the Black Sea, which is showed significantly low salinity between 18‰ and 22‰. This study suggested that lowered salinities does not appear to affect $U^{K'}_{37}$ temperature. These studies indicate that salinity does not affect alkenone temperature. Recently, however,

Rosell-Melé (1998) estimated the effect of salinity and temperature in the relative abundance of 37:4 to the total abundance of C_{37} alkenones (37:4%) using the alkenone sediment data from the Nordic seas and North Atlantic. This study suggested the influence of salinity on the $U^{K'}_{37}$ index. According to Rosell-Melé (1998), a lower salinity appears to produce a higher abundance of 37:4%, and the percentage of $C_{37:4}$ alkenone in the total C_{37} alkenones (37:4%) is high (> 5) below ~6℃. If the relationship between 37:4% and salinity found by Rosell-Melé (1998) is valid for the East Sea, a high 37:4% content should be observed for the sediment samples in the glacial period. Therefore, 37:4% values in 05PC-14, 05PC-15, and 05PC-23 were calculated (Fig. 22). Evidently, 37:4% values for these cores are lower than 5, suggesting that the SST cannot be so low. In the view of Rosell-Melé (1998), SSTs of 05PC-14, 05PC-15, and 05PC-23 must have been at least higher than ~6℃. However, since there is no direct evidence of abruptly high alkenone temperature during glacial period, a salinity effects on alkenone-SSTs are still unlikely. Further research about a salinity effects on alkenone-SSTs is necessary.

The third possibility is an effect of nutrient concentration and growth rate on alkenone-SSTs. According to previous studies, the nutrient concentration impact on $U^{K'}_{37}$ is uncertain. Popp et al. (1998) present the results of $U^{K'}_{37}$ from *E. huxleyi* grown in chemostat cultures at constant temperature but at variable growth rates. This study concluded that nutrient-limited growth rate effects will not produce serious errors in paleotemperature determinations using $U^{K'}_{37}$. On the other hand, Epstain et

al. (1998) determined that the isothermal culturing experiments with *E. huxleyi* clone CCMP372 show $U^{K'}_{37}$ values to also vary with nutrient availability and cell division rate. According to Epstain et al. (1998), when NO_x concentration drop from about 40 μM to < 1 μM, $U^{K'}_{37}$ increase from 0.10 to 0.19, which is increase of $U^{K'}_{37}$-based temperature from 1.8 to 4.4℃. In the view of Epstain et al. (1998), abruptly high alkenone temperature during the glacial period would have been caused by abrupt decrease of nutrient in the East Sea. The nutrient concentration in glacial period is unknown. Considering strong stratification of the water column during the glacial period would have limited the transport of nutrients from the deep to the surface, nutrient concentration would have still been low at the surface at that time. However, it is insufficient to conclude low nutrient concentration at the surface during the glacial period. Therefore, further research is necessary to define glacial-interglacial change in nutrient concentration.

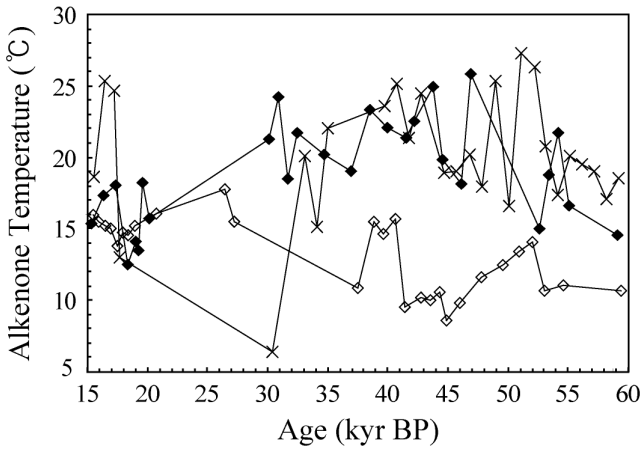

Fig 21. Comparison of alkenone temperature between 05PC-14(◇), 05PC-15(×) and 05PC-23(◆) during the glacial period between 15 and 60 kyr BP.

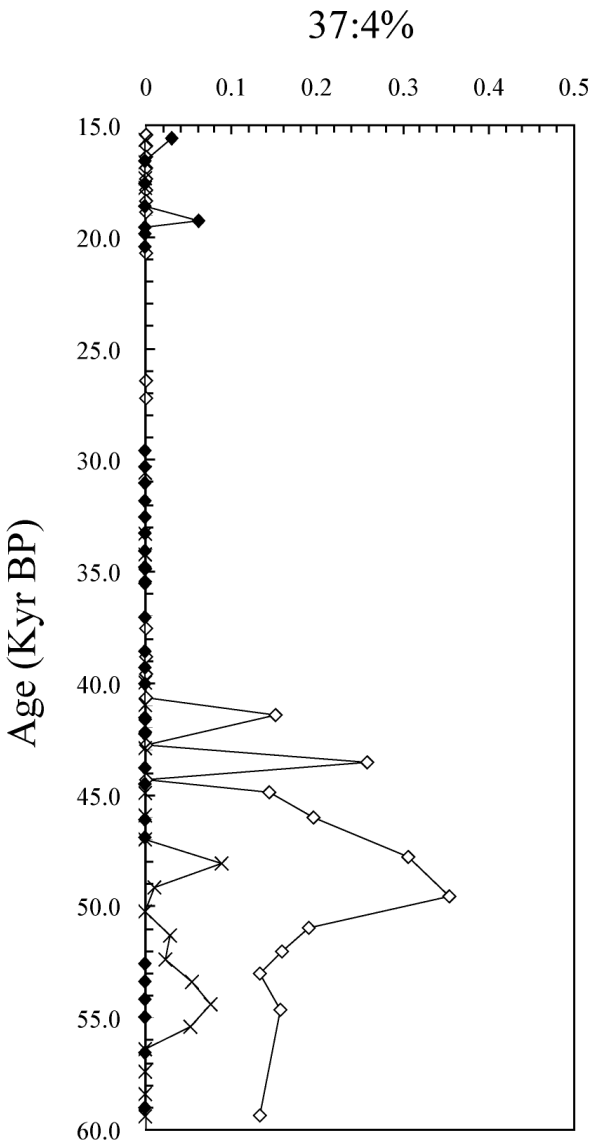

Fig 22. Variation in 37:4% values in core 05PC-14(◇), 05PC-15(×) and 05PC-23(◆) during the glacial period.

7. Conclusions

This study presents the alkenone records from the western margin of the East Sea for a period of 130 kyr BP. Our results are summarized as follows :

(1) The alkenone temperature of 05PC-14 fluctuated between 8.5℃ and 19.4℃ throughout the 80-kyr period, with the highest value (i.e. 19.4℃) occurring at 7.5 kyr BP and the lowest (i.e. 8.5℃) occurring at 44.9 kyr BP. The alkenone temperature of 05PC-15 fluctuated between 6.3℃ and 27.4℃ throughout the 110-kyr period, with the highest value (i.e. 27.4℃) occurring at 51.3 kyr BP and the lowest (i.e. 6.3℃) occurring at 30.6 kyr BP. The alkenone temperature of 05PC-23 fluctuated between 9.6℃ and 25.8℃ throughout the 130-kyr period, with the highest value (i.e. 25.8℃) occurring at 46.9 kyr BP and the lowest (i.e. 9.6℃) occurring at 62.4 kyr BP. The fluctuations of alkenone temperature were remarkably large during the last glacial period, between 30 and 60 kyr BP, in the study area of 05PC-15 and 05PC-23.

(2) For period of MIS 5, SST of MIS 5e was higher than those of present, SSTs of MISs 5c and d were close to those of present, and SSTs of MISs 5a and b were lower than those of present. It seems to be closely related to change of the East Asian monsoon system and global sea level changes, which influenced the warm water inflow into the East Sea. For period of MIS 4, the alkenone temperatures were very low. It seems to be

closely associated with a global sea level fall of 60-80m during this period, which restricted the inflow of the TWC into the East Sea. Also, the low SSTs were influenced by strong winter monsoon during this period. For period of MIS 3, some alkenone temperature were anomalously higher than MIS 1. Also, for period of MIS 2, some alkenone temperature were anomalously high. It have been reported previously for the East Sea, but it's not clear for what to be a major factor responsible for the anomalously warm alkenone temperature. Further studies are necessary. For period of MIS 1, alkenone temperature increased up to the present temperature in the early MIS 1. It seems to be closely related to global sea level changes, which influenced the warm water inflow into the East Sea during the mid MIS 1 (8-10 kyr BP), and change of the East Asian monsoon system.

(3) Warm alkenone temperature episodes occurred repeatedly in the glacial period between 15 and 60 kyr BP. Such warm alkenone temperature events in the MIS 3 have three possible causes. The first possibility is an effects of haptophyte species on alkenone-SSTs. The second possibility is a salinity effects on alkenone-SSTs. The third possibility is an effect of nutrient concentration and growth rate on alkenone-SSTs. These effects together could have caused anomalously warn alkenone temperatures in the MIS 3 in the study area of 05PC-15 and 05PC-23.

8. Reference

Berner, R.A., Raiswell, R., 1983, Burial of organic carbon and pyrite sulfur in sediments over Phanerozoic time: A new theory, *Geochim. Cosmochim. Acta*, 47, 855-862.

Brasell, S. C., Eglinton, G., Marlowe, I. T., Pflaumann, U., and Sarnthein, M., 1986, Molecular stratigraphy: a new tool for climatic assessment. *Nature*, 320, 129-133.

Conte, M.H., Thompson, A., Lesley, D., Harris, R.P., 1998, Generic and physiological influences on the alkenone/alkenoate versus growth temperature relationship in *Emiliania huxleyi* and *Gephyrocapsa oceanica*. *Geochimica et Cosmochimica Acta*, 62, 51-68.

Crusius, T., Pedersen, T.F., Calvert, S.E., Cowie, G.L., and Oba, T., 1999, A 36 kyr geochemical record from the sea of Japan of organic matter flux variations and changes in intermediate water oxygen isotope concentration. *Paleoceanography*, 14, 248-259.

Demasion, G.J., Moore, G.T., 1980, Anoxic environments and oil source bed genesis, *AAPG Bull.*, 64, 1179-1209.

Epstein, B.L., D'Hondt, S., Quinn, J.G., Zhang, J., Hargraves, P.E., 1998, An effect of dissolved nutrient concentrations on alkenone-based temperature estimates. *Paleoceanography*, 13, 122-126.

Fujine, K., 2004, fluctuation of the alkenone SST in the Japan Sea during the last 160 kys. PhD thesis, *University of Tokyo*, P156.

Fujine, K., Yamamoto, M., Tada, R., Kido, Y., 2006, Asalinity-related occurrence of a novel alkenone and alkenoate in late Pleistocene sediments from the Japan Sea. *Organic Geochemistry*, 37, 1074-7084.

Gorbarenko, S.A. and Southon, J.R., 2000, Detailed Japan Sea paleoceanography during the last 25 kyr: constraints from AMS dating and δ18O of planktonic foraminifera. *Palaeogeography Palaeoclimatology Palaeoecology*, 156, 177-193.

Grootes, P.M., Stuiver, M., 1997, Oxygen 18/16 variability in Greenland snow and ice with 10^3 to 10^5-year time resolution. *J. Geophys. Res.*, 102, 26455-26470.

Harada, N., Ahagon, N., Sakamoto, T., Uchida, M., Ikehara, M., Shibata, Y., 2006, Rapid fluctuation of alkenone temperature in the southwestern Okhotsk Sea during the Past 120 kyr. *Global and Planetary Changes.*, 53, 29-46.

Ikehara, K., 2003, Late Quaternary seasonal sea-ice history of the northeastern Japan Sea. *J. Oceanogr*, 59, 585-593.

Ikehara, H., Itaki, T., 2007, Millennial-scale fluctuations in seasonal sea-ice and deep-water formation in the Japan Sea during the late Quaternary. *Palaeogoegraphy, Palaeoclimatology, Palaeoecology*, 247, 131-143.

Irino, T., Tada, R., 2002, High-resolution reconstruction of variation in

aeolian dust (Kosa) deposition at ODP site 797, the Japan Sea, during the last 200 ka. *Global and Planetary Change*, 35, 143-156.

Ishiwatari, R., Houtatsu, M., and Okada, H., 2001, Alkenone-sea surface temperatures in the Japan Sea over the past 36 kyr: warm temperatures at the last glacial maximum. *Organic Geochemistry*, 32, 57-67.

Isobe, A. and Isoda, Y., 1997, Circulation in the Japan Basin, the northern part of the Japan Sea. *J. Oceanogr.*, 53, 373-381.

Jian, Z., Wang, P., Saito, Y., Wang, J., Pflaumann, U., Oba, T., Cheng, X., 2000, Holocene variability of the Kuroshio Current in the Okinawa Trough, northwestern Pacific Ocean. *Earth and Planetary Science Letters*, 184, 305-319.

Keigwin, W.D. and Gorbarenko, S.A., 1992, Sea level, surface salinity of the Japan Sea, and the Youger Dryas event in the northwestern Pacific Ocean. *Quaternary Research*, 37, 346-360.

Kido, Y., Minami, I., Tada, R., Fujine, K., Irino, T., Ikehara, K., and Chun, J.H., 2007, Orbital-scale stratigraphy and high-resolution analysis of biogenic components and deep water oxygenation conditions in the Japan sea during the last 640 kyrs using XRF microscanner. *Palaeogeography Palaeoclimatology Palaeoecology*, 247, 32-49.

KIGAM Report, 2004, Study on Earth's Environmental Change Using Quaternary Sedimentary Records : Phase Ⅰ.

Lambeck, K., Yakoyama, Y., and Purcell, A., 2002, Into and out of Last Glacial Maximum: sea-level change during the oxygen isotope Stage 3 and 2. *Quaternary Science Reviews*, 21, 343-360.

Lee, K.E. and Schneider, R., 2005, Alkenone production in the upper 200m of the Pacific Ocean. *Deep-Sea Research I*, 52, 443-456.

Lee, K.E., 2007, Surface water changes recorded in Late Quaternary marine sediments of the Ulleung Basin, East Sea (Japan Sea). *Palaeogeography Palaeoclimatology Palaeoecology*, 247, 18-31.

Lee, K.E., Bahk, J.J., Choi, J.Y., 2008, Alkenone temperature estimates for the East Sea during the last 190,000 years. *Organic Geochemistry*, 39, 741-753.

Leventhal, J.S., 1983, An interpretation of carbon and sulfur relationships in Black Sea sediments as indicators of environments of deposition, *Geochim. Cosmochim. Acta*, 47, 133-137.

Machida, H., 1999, The stratigraphy, chronology and distribution of distal marker-tephra in and around Japan. *Global Planetary Change*, 21, 71-94.

Marlowe, I.T., Brassell, S.C., Eglinton, G., Green, J.C., 1990, Long-chain alkenones and alkyl alkenoates and the fossil coccolith record of marine sediments. *Chemical Geology*, 88, 349-375.

Masuzawa, T. and Kitano, Y., 1984, Appeatance of H_2S-bearing bottom waters during the last glacial period in the Japan Sea. *Geochemecal Journal*, 18, 167-172.

Moore, T.C., Burckle, L.H., Geitzenauer, K., Luz, B., Molina-Cruz, A., Robertson, J.H., Sachs, H., Sancetta, C., Thompson, P., Wenkam, C., 1980, The reconstruction of sea surface temperatures in the Pacific Ocean. *Marine Micropaleontology*, 5, 215-247.

Müller, P. J., Kirst, G., Ruhland, G., Storch, I. V., and Rosell-Mele, A., 1998, Calibration of the alkenone paleotemperature index $U^{K'}_{37}$ based on core-tops from the eastern South Atlantic and global ocaen(60°N-60°S). *Geochim. Cosmochim. Acta*, 52, 1757-1771.

Nakagawa, T., Kitagawa, H., Yasuda, Y., Taraso, v.P.E., Nishida, K., Gotanda, K., Sawai, Y.Yangtze River Civilization Program Members, 2003, Asynchronous climate changes in the north Atlantic and Japan during the last termination. *Science*, 299, 688-691.

Oba, T., Kato, M., Kitazato, H., Koizumi, I., Omura, A., Sakai, T., and Takayama, T., 1991, Paleoenvironmental changes in the Japan Sea during the last 85,000 years. *Paleoceanography*, 6, 499-518.

Oba, T., Murayama, M., Matsumoto, E., and Nakamura, T.,1995, AMS-^{14}C Ages of Japan Sea cores from the Oki Ridge. *The Quaternary*

Research (in Japanese with English Abstract), 34, 289-296.

Popp, B.N., Kenig, F., Wakeham, S.G., Laws, E.A., Bidigare, R.R., 1998, Does growth rate affect ketone unsaturation and intracellular carbon isotopic variability in *E. huxleyi*? *Paleoceanography*, 13, 35-41.

Prahl, F.G. and Wakeham, S.G., 1987, Calibration of unsaturation patternsin long-chain ketone compositions for palaeotemperature assessment. *Nature*, 30, 367-369.

Prahl, F.G., Muehlhausen, L.A., and Zahnle, D.L., 1988, Further evaluation of long-chain alkenones as indicators of paleoceanographic conditions. *Geochim. Cosmochim. Acta*., 52, 2303-2310.

Rosell-Melé, A., 1998, Interhemispheric appraisal of the value of alkenone indices as temperature and salinity proxies in high-latitude locations. *Paleoceanography*, 13, 694-703.

Rosell-Melé, A., Comes, P., Muller, P. J., and Ziveri, P., 2000, Alkenone fluxes and anomalous $U^{K'}_{37}$ values during 1989-1990 in the Northeast Atlantic(48°N 21°W). *Marine Chemistry*, 71, 251-264.

Ryu, E.Y., Yi, S.H., Lee, S.J., 2005, Late Pleistocene-Holocene paleoenvitonmental changes inferred from the diatom record of the Ulleung Basin, East Sea (Sea of Japan). *Marine Micropaleotology*, 55, 157-182.

Sawada, K., Handa, N., Shiraiwa, Y., Danbara, A., Montani, S., 1996, Long-chain alkenones and alkyl alkenoates in a coastal and pelagic sediments of the northwest North Pacific, with special reference to the reconstruction of *Emiliania huxleyi* and *Gephyrocapsa oceanica* ratios. *Organic Geochimistry*, 24, 751-764.

Sikes, E.L., Farrington, J.W., Keigwin, L.D., 1991, Use of the alkenone unsaturation ratio UK37 to determine past sea surface temperatures: core-top SST calibrations and methodology consideration. *Earth and Planetary Science Letters*, 104, 36-47.

Senjyu, T., and Sudo, H., 1994, The upper portion of Japan Sea proper Water. Its source and circulation as deduced from isopycnal analysis. *J. Oceanogr. Soc. Japan*, 50, 663-690.

Sonzogni, C., Bard, E., Rostek, F., Dollfus, D., 1997, Temperature and salinity effects on alkenone ratios measured in surface sediments from the Indian Ocean. *Quaternary Research*, 47, 344-355.

Tada, R., Irino, T., Koizumi, I., 1995, Possible Dansgaard-Oeschger oscillation signal recorded in the Japan Sea sediments. In: Tsunogai, S., Iseki, K., Koike, I., Oba, T. (Eds.), Global Fluxes of Carbon and its Related Substances in the Coastal Sea-Ocean-Atmosphere System. Proc. 1994 Sapporo IGBP Symp., M&J International, Yokohama, pp. 517-522.

Tada, R., Irino, T., and Koizumi, I., 1999, Land-ocean linkages over orbital and millennial timescale recorded in late Quaternary sediments of the Japan Sea. *Paleoceanography*, 14, 236-247.

Volkman, J.K., Barrett, S.M., Blankburn, S.I., Sikes, E.L., 1995, Alkenones in *Gephyrocapsa oceanica* : Implications for studies of paleoclimate. *Geochimica et Cosmochimica Acta*, 59, 513-520.

Waelbroeck, C., Labeyrie, L., Michel, E., Duplessy, J.C., McManus, J.F., Lambeck, K., Balbon, E., Labracherie, M., 2002, Sea-level and deep water temperature changes derived from benthic foraminifera isotopic records. *Quaternary Science Reviews*, 21, 295-305.

Wang, L., Oba, T., 1998, Tele-connections between East Asian monsoon and the high-latitude climate: a comparison between the GISP2 ice core record and the high resolution marine records from the Japan and the South China Seas. *The Quat. Res.* (Daiyonkikenkyu), 37, 211-219.

Wang, P., Clemens, S., Beaufort, L., Braconnot, P., Ganssen, G., Jian, Z., Kershaw, P., Sarnthein, M., 2005, Evolution and variability of the Asian monsoon system: state of the art and outstanding issues. *Quaternary Science Reviews*, 24, 595-629.

Webster, P.J., 1987, The elementary monsoon. In: Fein, J.S. and Stephens,

P.L. (Eds.), Monsoons, Wiley-Interscience, New York, pp. 1-32.

Yokoyama, Y., Kido, Y., Tada, R., Minami, I., Finkel, R.C., Matsuzaki, H., 2007, Japan Sea oxygen isotope stratigraphy and global sea-level changes for the last 50,000years recorded in sediment core from the Oki ridge. *Palaeogeography Palaeoclimatology Palaeoecology*, 247, 5-17.

Yasunari, T., 1991, Role of the Asian monsoon in the global climate system. *Mon. Kagaku*, 61, 697-704.

Zhang, X.Y., Lu, H.Y., Arimoto, R., Gong, S.L., 2002, Atmospheric dust loadings and their relationship to rapid oscillations of the Asian winter monsoon climate: two 250-kyr loess records. *Earth and Planetary Science Ltters*, 202, 637-643.

Appendix 1.

Alkenone analysis data of core 05PC-14

Depth (cm)	Age (kyr)	$C_{37:4}$ (μg/g)	$C_{37:3}$ (μg/g)	$C_{37:2}$ (μg/g)	Total (μg/g)	$U^{K'}_{37}$	$U^{K'}_{37}T$ (℃)
0	0.0	0.0	0.8	1.5	2.4	0.6531	18.1
3	0.3	0.0	1.0	1.4	2.4	0.5678	15.6
6	0.6	0.0	0.3	0.6	0.9	0.6199	17.1
10	1.0	0.0	1.5	2.0	3.4	0.5770	15.8
15	4.5	0.0	1.4	1.9	3.3	0.5756	15.8
20	2.0	0.0	1.2	1.6	2.9	0.5683	15.6
25	2.5	0.0	0.7	1.1	1.8	0.5896	16.2
30	3.0	0.0	1.0	1.4	2.4	0.5851	16.1
35	3.5	0.0	1.2	1.8	2.9	0.5986	16.5
40	4.0	0.0	0.5	0.7	1.2	0.5533	15.1
45	4.5	0.0	0.7	1.0	1.7	0.5762	15.8
50	5.0	0.0	0.6	0.9	1.5	0.6104	16.8
55	5.5	0.0	0.7	1.1	1.9	0.6111	16.8
60	6.0	0.0	0.7	1.2	1.9	0.6298	17.4
65	6.5	0.0	0.4	0.7	1.2	0.6313	17.4
70	7.0	0.0	0.7	1.1	1.8	0.6181	17.0
75	7.5	0.0	0.4	0.9	1.2	0.7002	19.4
80	8.0	0.0	0.4	0.8	1.2	0.6615	18.3
85	8.5	0.0	0.8	1.1	1.9	0.5849	16.1
90	9.0	0.0	0.9	1.3	2.3	0.5809	15.9
95	9.5	0.0	0.9	1.3	2.2	0.5979	16.4
100	9.9	0.0	1.4	1.9	3.3	0.5800	15.9
105	10.4	0.0	1.4	1.9	3.3	0.5716	15.7
110	10.9	0.0	1.6	2.0	3.6	0.5687	15.6
115	11.4	0.0	1.7	2.1	3.8	0.5627	15.4
120	11.9	0.0	1.7	2.0	3.7	0.5474	15.0
125	12.4	0.0	1.7	1.9	3.6	0.5341	14.6
130	12.9	0.0	1.2	1.6	2.8	0.5598	15.3
135	13.4	0.0	1.2	1.7	2.9	0.5769	15.8
140	13.9	0.0	0.8	1.1	1.9	0.5828	16.0
145	14.4	0.0	1.8	2.2	4.0	0.5418	14.8
150	14.9	0.0	2.1	2.6	4.7	0.5446	14.9
155	15.4	0.0	1.2	1.6	2.8	0.5806	15.9
160	15.9	0.0	1.4	1.8	3.2	0.5665	15.5

Appendix 1. (*continued*)

Depth (cm)	Age (kyr)	$C_{37:4}$ (μg/g)	$C_{37:3}$ (μg/g)	$C_{37:2}$ (μg/g)	Total (μg/g)	$U^{K'}_{37}$	$U^{K'}_{37}T$ (℃)
175	17.4	0.0	0.3	0.3	0.5	0.5089	13.8
180	17.9	0.0	0.3	0.4	0.7	0.5409	14.8
185	18.4	0.0	0.1	0.1	0.3	0.5328	14.5
190	18.9	0.0	0.1	0.1	0.1	0.5556	15.2
192	20.7	0.0	0.0	0.1	0.1	0.5842	16.0
207	26.5	0.0	0.0	0.0	0.0	0.6430	17.8
210	27.2	0.0	0.0	0.0	0.0	0.5667	15.5
245	37.5	0.0	0.1	0.1	0.1	0.4053	10.8
250	38.8	0.0	0.0	0.0	0.0	0.5660	15.5
253	39.6	0.0	0.0	0.0	0.1	0.5382	14.7
257	40.7	0.0	0.0	0.0	0.1	0.5713	15.7
260	41.4	0.1	0.2	0.1	0.4	0.3627	9.5
265	42.7	0.0	0.2	0.1	0.4	0.3835	10.1
268	43.5	0.1	0.2	0.1	0.4	0.3778	10.0
271	44.3	0.0	0.0	0.0	0.1	0.3957	10.5
275	44.9	0.0	0.1	0.0	0.1	0.3287	8.5
280	46.0	0.0	0.1	0.1	0.2	0.3697	9.7
285	47.8	0.1	0.2	0.1	0.4	0.4329	11.6
290	49.6	0.1	0.1	0.1	0.3	0.4630	12.5
294	51.0	0.6	1.3	1.3	3.3	0.4958	13.4
297	52.0	0.0	0.1	0.1	0.3	0.5173	14.1
300	53.0	0.1	0.2	0.2	0.5	0.3990	10.6
305	54.6	0.1	0.3	0.2	0.6	0.4144	11.0
320	59.4	0.1	0.2	0.1	0.4	0.3994	10.6
325	61.0	0.1	0.3	0.2	0.5	0.4119	11.0
330	62.7	0.0	0.0	0.0	0.1	0.4708	12.7
335	64.7	0.0	0.2	0.1	0.3	0.4523	12.2
340	66.8	0.0	0.3	0.2	0.5	0.4363	11.7
345	68.8	0.1	1.0	0.7	1.9	0.4276	11.4
352	71.5	0.0	2.2	1.9	4.1	0.4676	12.6
355	72.3	0.1	2.1	1.9	4.1	0.4753	12.8
360	73.7	0.0	2.1	2.0	4.1	0.4944	13.4
366	75.0	0.1	0.3	0.3	0.7	0.5295	14.4
370	75.8	0.0	3.5	4.8	8.4	0.5757	15.8
372	76.2	0.3	0.3	0.4	1.0	0.6050	16.6

Appendix 2.

Alkenone analysis data of core 05PC-15

Depth (cm)	Age (kyr)	C37:4 (μg/g)	C37:3 (μg/g)	C37:2 (μg/g)	total (μg/g)	$U^{K'}_{37}$	$U^{K'}_{37}$ (˚C)
0	0.0	0.0	0.0	0.0	0.1	0.6573	18.2
5	0.7	0.0	0.1	0.2	0.3	0.6291	17.4
10	1.4	0.0	0.1	0.2	0.3	0.6200	17.1
15	2.0	0.0	0.0	0.1	0.1	0.6347	17.5
20	2.8	0.0	0.0	0.1	0.1	0.6244	17.2
25	3.6	0.0	0.0	0.1	0.1	0.6038	16.6
30	4.1	0.0	0.0	0.1	0.1	0.5998	16.5
35	4.8	0.0	0.1	0.1	0.1	0.5783	15.9
40	5.7	0.0	0.1	0.1	0.2	0.5993	16.5
45	6.4	0.0	0.2	0.3	0.4	0.5950	16.4
55	7.5	0.0	0.0	0.1	0.1	0.6163	17.0
60	8.5	0.0	0.2	0.2	0.4	0.5797	15.9
70	10.0	0.0	0.1	0.1	0.2	0.6328	17.5
75	10.7	0.0	0.2	0.2	0.4	0.5653	15.5
80	11.4	0.0	0.1	0.2	0.3	0.5900	16.2
85	12.1	0.0	0.2	0.2	0.4	0.5725	15.7
90	12.8	0.0	0.3	0.3	0.6	0.5530	15.1
95	13.5	0.0	0.2	0.3	0.5	0.6038	16.6
100	14.2	0.0	0.1	0.1	0.2	0.6008	16.5
105	14.9	0.0	0.1	0.3	0.4	0.7748	21.6
110	15.6	0.0	0.0	0.1	0.1	0.6729	18.6
117	16.6	0.0	0.1	1.2	1.3	0.9041	25.4
122	17.3	0.0	0.1	0.6	0.6	0.8789	24.7
125	17.8	0.0	0.0	0.0	0.0	0.4823	13.0
265	30.6	0.0	0.0	0.0	0.0	0.2538	6.3
280	33.3	0.0	0.0	0.0	0.1	0.7244	20.2
285	34.2	0.0	0.0	0.0	0.1	0.5540	15.1
290	35.2	0.0	0.0	0.1	0.1	0.7887	22.1
315	40.0	0.0	0.0	0.1	0.1	0.8429	23.6
320	41.0	0.0	0.0	0.0	0.0	0.8978	25.3
325	42.0	0.0	0.0	0.0	0.0	0.7684	21.5
330	43.0	0.0	0.0	0.0	0.0	0.8747	24.6
340	45.0	0.0	0.0	0.0	0.0	0.6832	18.9
345	46.0	0.0	0.0	0.0	0.0	0.6862	19.0

Appendix 2. (*continued*)

Depth (cm)	Age (kyr)	C37:4 (μg/g)	C37:3 (μg/g)	C37:2 (μg/g)	total (μg/g)	$U^{K'}_{37}$	$U^{K'}_{37}$ (˚C)
350	47.0	0.0	0.0	0.0	0.1	0.7264	20.2
355	48.1	0.0	0.0	0.0	0.1	0.6512	18.0
360	49.2	0.0	0.0	0.2	0.2	0.9016	25.4
365	50.3	0.0	0.0	0.1	0.1	0.6055	16.7
370	51.3	0.0	0.0	1.1	1.2	0.9690	27.4
375	52.4	0.0	0.0	0.6	0.7	0.9355	26.4
380	53.4	0.0	0.0	0.1	0.1	0.7480	20.9
385	54.4	0.0	0.0	0.1	0.1	0.6307	17.4
390	55.4	0.0	0.1	0.1	0.2	0.7241	20.2
395	56.4	0.0	0.0	0.1	0.1	0.7050	19.6
400	57.4	0.0	0.0	0.0	0.1	0.6879	19.1
405	58.4	0.0	0.0	0.0	0.1	0.6196	17.1
410	59.4	0.0	0.0	0.0	0.0	0.6719	18.6
415	60.4	0.0	0.0	0.0	0.1	0.6032	16.6
420	61.4	0.0	0.0	0.0	0.0	0.5046	13.7
425	62.4	0.0	0.0	0.0	0.1	0.5052	13.7
430	63.4	0.0	0.1	0.1	0.2	0.6842	19.0
435	64.2	0.0	0.0	0.0	0.0	0.5452	14.9
440	64.9	0.0	0.0	0.0	0.1	0.4930	13.4
445	65.7	0.0	0.0	0.0	0.1	0.5017	13.6
450	66.5	0.0	0.0	0.0	0.1	0.4592	12.4
455	67.2	0.0	0.0	0.0	0.0	0.4915	13.3
460	68.0	0.0	0.0	0.0	0.1	0.4757	12.8
465	68.7	0.0	0.0	0.0	0.0	0.4743	12.8
470	69.5	0.0	0.0	0.0	0.1	0.4803	13.0
475	70.3	0.0	0.0	0.0	0.1	0.4974	13.5
480	71.5	0.0	0.2	0.2	0.4	0.5110	13.9
485	72.6	0.0	0.2	0.3	0.5	0.5071	13.8
490	73.7	0.0	0.2	0.2	0.4	0.5418	14.8
495	74.8	0.0	0.1	0.1	0.1	0.5023	13.6
500	76.0	0.0	0.0	0.0	0.1	0.5126	13.9
505	77.1	0.0	0.1	0.1	0.1	0.5074	13.8
510	78.5	0.0	0.1	0.1	0.2	0.5066	13.8
515	81.1	0.0	0.4	0.5	0.9	0.5482	15.0
520	83.6	0.0	0.4	0.4	0.8	0.5410	14.8

Appendix 2. (*continued*)

Depth (cm)	Age (kyr)	C37:4 (μg/g)	C37:3 (μg/g)	C37:2 (μg/g)	total (μg/g)	$U^{K'}_{37}$	$U^{K'}_{37}$ (˚C)
525	86.2	0.0	0.2	0.3	0.4	0.5779	15.8
530	87.3	0.0	0.1	0.1	0.2	0.5319	14.5
535	88.3	0.0	0.1	0.1	0.2	0.5217	14.2
540	89.4	0.0	0.1	0.1	0.2	0.5454	14.9
545	90.4	0.0	0.3	0.4	0.7	0.5634	15.4
550	91.5	0.0	0.2	0.3	0.5	0.6240	17.2
555	92.5	0.0	0.3	0.6	0.8	0.6753	18.7
560	93.6	0.0	0.3	0.4	0.8	0.5653	15.5
565	94.6	0.0	0.4	0.5	0.9	0.5223	14.2
570	95.6	0.0	0.7	0.9	1.6	0.5836	16.0
575	96.7	0.0	0.6	0.7	1.3	0.5495	15.0
580	97.7	0.0	0.5	0.6	1.2	0.5199	14.1
585	98.8	0.0	0.7	2.0	2.7	0.7464	20.8
590	99.8	0.0	0.6	1.2	1.8	0.6637	18.4
595	100.9	0.0	0.5	1.1	1.6	0.6866	19.0
600	101.9	0.0	0.2	0.9	1.1	0.8315	23.3
605	103.0	0.0	0.1	0.2	0.3	0.7558	21.1
610	104.0	0.0	0.1	0.1	0.2	0.5247	14.3
615	105.0	0.0	0.1	0.1	0.1	0.5202	14.2
625	107.1	0.0	0.0	0.1	0.1	0.5705	15.6
630	108.2	0.0	0.1	0.2	0.3	0.6985	19.4
635	109.1	0.0	0.2	0.4	0.6	0.7254	20.2
640	109.4	0.0	0.2	0.8	1.0	0.7971	22.3
645	109.7	0.0	0.2	0.4	0.6	0.6046	16.6
650	110.0	0.0	0.3	0.5	0.9	0.6126	16.9
655	110.3	0.0	0.3	0.4	0.7	0.6269	17.3
660	110.6	0.0	0.2	0.4	0.6	0.6543	18.1

Appendix 3.
Alkenone analysis data of core 05PC-23

Depth (cm)	Age (kyr)	$C_{37:4}$ (μg/g)	$C_{37:3}$ (μg/g)	$C_{37:2}$ (μg/g)	Total (μg/g)	$U^{K'}_{37}$	$U^{K'}_{37}T$ (℃)
0	0.0	0.0	0.0	0.0	0.1	0.5940	16.3
2	1.0	0.0	1.4	1.8	3.2	0.5717	15.7
4	2.0	0.0	0.0	0.0	0.1	0.6307	17.4
6	3.0	0.0	0.3	0.5	0.8	0.6117	16.8
8	4.0	0.0	0.0	0.0	0.1	0.6373	17.6
10	5.1	0.0	0.8	1.2	2.1	0.5967	16.4
12	6.1	0.0	0.0	0.0	0.1	0.6199	17.1
14	7.1	0.0	0.8	1.2	2.1	0.5997	16.5
16	8.2	0.0	0.0	0.0	0.0	0.5911	16.2
18	9.2	0.0	0.8	1.1	1.9	0.5869	16.1
20	10.2	0.0	0.0	0.0	0.0	0.6344	17.5
22	11.2	0.0	0.5	0.8	1.3	0.6051	16.6
26	13.3	0.1	0.8	1.1	1.9	0.5889	16.2
28	14.3	0.0	0.1	0.1	0.1	0.5917	16.3
30	15.3	0.1	1.7	2.1	3.9	0.5624	15.4
32	16.3	0.0	0.0	0.0	0.1	0.6292	17.4
34	17.3	0.0	1.5	2.8	4.3	0.6535	18.1
36	18.4	0.0	0.0	0.0	0.1	0.4649	12.5
38	19.0	0.1	0.7	0.7	1.5	0.5178	14.1
40	19.3	0.0	0.0	0.0	0.0	0.4961	13.4
42	19.6	0.0	0.1	0.3	0.4	0.6591	18.2
46	20.2	0.0	0.1	0.1	0.1	0.5718	15.7
112	30.1	0.0	0.1	0.3	0.3	0.7615	21.2
116	30.9	0.0	0.0	0.2	0.2	0.8627	24.2
120	31.7	0.0	0.1	0.1	0.2	0.6689	18.5
124	32.4	0.0	0.1	0.4	0.5	0.7753	21.7
136	34.7	0.0	0.4	1.0	1.4	0.7240	20.1
148	37.0	0.0	0.0	0.1	0.1	0.6867	19.0
156	38.5	0.0	0.2	0.8	0.9	0.8308	23.3
164	40.0	0.0	0.2	0.8	1.0	0.7894	22.1
172	41.5	0.0	0.0	0.1	0.2	0.7660	21.4
176	42.3	0.0	0.1	0.3	0.4	0.8032	22.5
184	43.8	0.0	0.3	2.0	2.2	0.8845	24.9
188	44.5	0.0	0.2	0.5	0.7	0.7123	19.8

Appendix 3. (*continued*)

Depth (cm)	Age (kyr)	$C_{37:4}$ (μg/g)	$C_{37:3}$ (μg/g)	$C_{37:2}$ (μg/g)	Total (μg/g)	$U^{K'}_{37}$	$U^{K'}_{37}T$ (℃)
196	46.1	0.0	0.2	0.4	0.6	0.6538	18.1
200	46.9	0.0	0.5	5.0	5.5	0.9153	25.8
228	52.6	0.0	0.2	0.2	0.4	0.5490	15.0
232	53.4	0.0	0.3	0.6	0.9	0.6760	18.7
236	54.2	0.0	0.3	1.0	1.2	0.7773	21.7
240	55.0	0.0	0.5	0.7	1.1	0.6030	16.6
260	59.1	0.0	0.3	0.3	0.6	0.5352	14.6
272	61.6	0.0	0.1	0.1	0.2	0.3817	10.1
274	62.0	0.0	0.1	0.1	0.2	0.3830	10.1
276	62.4	0.0	0.2	0.1	0.3	0.3651	9.6
280	63.2	0.0	0.1	0.1	0.2	0.4129	11.0
284	64.0	0.0	0.2	0.1	0.3	0.3810	10.1
288	64.8	0.0	0.1	0.1	0.2	0.4324	11.6
292	65.6	0.0	0.1	0.0	0.1	0.4557	12.3
296	66.4	0.0	0.1	0.1	0.2	0.4357	11.7
300	67.3	0.0	0.1	0.0	0.1	0.4356	11.7
304	68.1	0.0	0.1	0.1	0.2	0.4312	11.5
306	68.5	0.0	0.0	0.0	0.0	0.5147	14.0
308	68.9	0.0	0.1	0.1	0.2	0.4577	12.3
310	69.3	0.0	0.0	0.0	0.0	0.5180	14.1
316	70.5	0.0	1.3	1.7	2.9	0.5716	15.7
322	71.7	0.0	0.1	0.1	0.2	0.6562	18.2
326	72.6	0.0	0.5	0.4	1.0	0.4130	11.0
330	73.4	0.0	0.5	0.4	1.0	0.4175	11.1
332	73.8	0.7	1.3	1.7	3.8	0.5575	15.3
336	74.6	0.4	0.5	0.4	1.4	0.4587	12.3
338	75.0	0.0	0.4	0.6	1.1	0.5940	16.3
342	76.1	0.0	1.0	0.6	1.6	0.3893	10.3
346	77.2	0.0	0.2	0.1	0.2	0.3851	10.2
350	78.3	0.0	0.2	0.2	0.4	0.4408	11.8
354	79.4	0.1	1.1	1.0	2.1	0.4718	12.7
366	82.6	0.1	2.9	2.5	5.5	0.4580	12.3
368	83.2	0.0	4.0	3.6	7.6	0.4731	12.8
372	84.3	0.0	6.3	4.8	11.1	0.4305	11.5
374	84.8	0.0	4.5	4.5	8.9	0.5000	13.6

Appendix 3. (*continued*)

Depth (cm)	Age (kyr)	$C_{37:4}$ (μg/g)	$C_{37:3}$ (μg/g)	$C_{37:2}$ (μg/g)	Total (μg/g)	$U^{K'}_{37}$	$U^{K'}_{37}T$ (℃)
376	85.4	0.0	4.7	3.8	8.6	0.4477	12.0
378	85.9	0.0	2.5	3.2	5.8	0.5583	15.3
380	86.5	0.0	0.6	0.5	1.1	0.4744	12.8
384	87.6	0.0	0.8	0.9	1.7	0.5478	15.0
386	88.1	0.0	0.2	0.1	0.3	0.4106	10.9
388	88.6	0.1	0.3	0.3	0.6	0.5226	14.2
392	89.7	0.0	0.2	0.2	0.5	0.5172	14.1
394	90.2	0.0	0.3	0.2	0.5	0.3700	9.7
396	90.6	0.0	1.3	1.6	2.8	0.5518	15.1
398	91.0	0.0	2.2	1.3	3.5	0.3784	10.0
400	91.5	0.0	1.5	2.3	3.8	0.6072	16.7
402	91.9	0.0	4.7	3.5	8.2	0.4268	11.4
406	92.7	0.0	1.8	1.2	3.0	0.4041	10.7
408	93.1	0.0	4.5	6.5	11.0	0.5878	16.1
410	93.6	0.0	2.3	1.6	3.9	0.4218	11.3
414	94.4	0.0	2.3	2.7	5.0	0.5378	14.7
416	94.8	0.0	2.6	3.8	6.3	0.5954	16.4
418	95.2	0.1	1.7	2.7	4.5	0.6057	16.7
420	95.6	0.0	0.5	0.8	1.3	0.6153	17.0
424	96.5	0.0	1.3	2.3	3.6	0.6330	17.5
426	96.9	0.1	1.2	2.1	3.4	0.6507	18.0
428	97.3	0.0	1.6	2.9	4.5	0.6528	18.1
430	97.7	0.0	1.4	2.5	4.0	0.6367	17.6
432	98.1	0.0	1.6	2.8	4.4	0.6457	17.8
434	98.6	0.0	1.1	2.1	3.2	0.6513	18.0
436	99.0	0.0	1.3	2.3	3.6	0.6309	17.4
440	99.8	0.0	0.9	1.4	2.4	0.6054	16.7
444	100.6	0.0	0.4	0.7	1.1	0.6032	16.6
448	101.5	0.0	0.7	1.0	1.8	0.5761	15.8
452	102.3	0.0	0.6	0.9	1.6	0.5846	16.0
456	103.2	0.0	0.4	0.5	0.8	0.5718	15.7
460	104.0	0.0	0.7	0.8	1.5	0.5439	14.8
464	104.8	0.0	1.1	1.4	2.5	0.5600	15.3
468	105.7	0.0	0.9	1.2	2.2	0.5610	15.4
472	106.5	0.0	0.2	0.3	0.5	0.5914	16.2

Appendix 3. (*continued*)

Depth (cm)	Age (kyr)	$C_{37:4}$ (μg/g)	$C_{37:3}$ (μg/g)	$C_{37:2}$ (μg/g)	Total (μg/g)	$U^{K'}_{37}$	$U^{K'}_{37}T$ (℃)
476	107.3	0.0	0.5	0.7	1.2	0.5877	16.1
480	108.2	0.0	0.4	0.7	1.1	0.5946	16.3
484	109.0	0.0	1.2	1.8	3.0	0.5915	16.3
486	109.4	0.0	0.1	0.1	0.2	0.5671	15.5
488	109.8	0.0	2.2	2.8	5.0	0.5674	15.5
490	110.2	0.0	5.0	7.8	12.8	0.6105	16.8
492	110.7	0.0	0.3	0.5	0.8	0.6167	17.0
494	111.1	0.0	0.7	0.9	1.5	0.5686	15.6
496	111.5	0.0	2.2	3.5	5.7	0.6192	17.1
498	111.9	0.0	0.4	0.5	1.0	0.5555	15.2
500	112.3	0.0	0.5	0.9	1.4	0.6515	18.0
502	112.7	0.0	2.5	4.5	7.0	0.6410	17.7
504	113.2	0.0	2.0	3.4	5.4	0.6322	17.4
506	113.6	0.0	4.6	8.2	12.8	0.6389	17.6
508	114.0	0.0	1.4	2.6	4.0	0.6477	17.9
510	114.4	0.0	1.3	2.5	3.8	0.6597	18.3
512	114.8	0.0	2.6	4.7	7.3	0.6482	17.9
514	115.2	0.0	1.2	2.3	3.5	0.6658	18.4
516	115.7	0.0	1.5	2.6	4.1	0.6433	17.8
518	116.1	0.0	2.2	4.3	6.4	0.6652	18.4
520	116.5	0.0	0.9	1.8	2.6	0.6695	18.5
522	116.8	0.0	1.5	2.9	4.4	0.6680	18.5
524	117.2	0.0	1.7	3.2	4.9	0.6528	18.1
526	117.5	0.0	1.4	3.2	4.7	0.6922	19.2
528	117.9	0.0	1.3	2.7	4.0	0.6849	19.0
530	118.2	0.0	1.0	2.2	3.2	0.6916	19.2
532	118.5	0.0	0.7	1.2	1.9	0.6470	17.9
536	119.2	0.0	0.3	0.7	1.0	0.7060	19.6
538	119.5	0.0	0.2	0.4	0.5	0.7148	19.9
542	120.2	0.0	0.3	0.7	1.0	0.7096	19.7
544	120.6	0.0	0.7	1.7	2.4	0.7033	19.5
546	120.9	0.0	0.3	0.8	1.1	0.7205	20.0
548	121.2	0.0	0.4	0.9	1.3	0.7225	20.1
550	121.6	0.0	0.5	1.3	1.9	0.7228	20.1
552	121.9	0.0	0.2	0.6	0.8	0.7336	20.4

Appendix 3. (*continued*)

Depth (cm)	Age (kyr)	$C_{37:4}$ (μg/g)	$C_{37:3}$ (μg/g)	$C_{37:2}$ (μg/g)	Total (μg/g)	$U^{K'}_{37}$	$U^{K'}_{37}T$ (℃)
554	122.2	0.0	5.3	14.4	19.7	0.7297	20.3
556	122.6	0.0	0.2	0.6	0.8	0.7302	20.3
558	122.9	0.0	1.8	4.5	6.3	0.7130	19.8
560	123.3	0.0	0.4	0.9	1.3	0.7127	19.8
562	123.6	0.0	1.3	3.0	4.4	0.6953	19.3
564	123.9	0.0	1.0	2.3	3.3	0.6836	19.0
566	124.3	0.0	1.1	2.5	3.6	0.6908	19.2
568	124.6	0.0	1.0	2.0	3.0	0.6724	18.6
570	124.9	0.0	1.5	3.3	4.9	0.6836	19.0
572	125.3	0.0	1.1	2.4	3.5	0.6836	19.0
574	125.6	0.0	0.5	1.2	1.7	0.7041	19.6
576	126.0	0.0	0.8	1.7	2.4	0.6884	19.1
578	126.3	0.0	0.4	1.0	1.4	0.7043	19.6
580	126.6	0.0	0.6	1.3	2.0	0.6834	19.0
582	127.0	0.0	0.4	1.0	1.4	0.6960	19.3
584	127.3	0.0	0.6	1.3	1.9	0.6804	18.9
586	127.6	0.0	0.3	0.8	1.1	0.7032	19.5
588	128.0	0.0	0.5	1.2	1.7	0.7020	19.5
592	128.7	0.0	0.4	1.0	1.4	0.7005	19.5
594	129.0	0.0	0.8	1.8	2.6	0.7099	19.7
596	129.3	0.0	0.5	1.1	1.5	0.6998	19.4
598	129.7	0.0	0.5	1.4	1.9	0.7295	20.3
600	130.0	0.0	0.1	0.3	0.4	0.7425	20.7
602	130.3	0.0	0.3	0.7	0.9	0.7233	20.1
604	130.7	0.0	0.3	0.7	1.1	0.6794	18.8
606	131.0	0.0	0.5	1.4	1.9	0.7408	20.6
608	131.4	0.0	0.0	0.1	0.2	0.7367	20.5

Acknowledgment

I express my special thanks to Prof. Lee for her discussions and critical review of my manuscript. I express my sincere thanks to the participants of the 2005 East Sea cruise on the R/V Tamhae Ⅱ for core recovery. Thanks also go to S.H. Lee for her help with sample preparation and alkenone analysis in the laboratory. I am grateful to Ryan Lee for his help with everything in the everywhere. I also appreciate to my friends H.Y. Seo, J.I. Park, H.Y. Jung, J.I. Lee, J.W. Kim, Y.H. Choi. Finally, my special thanks go to my parents and my younger brother, B.J. Choi.